ORIGINAL ARTICLE

Deficiency of *N*-acetylgalactosamine in *O*-linked Oligosaccharides of IgA Is a Novel Biologic Marker for Crohn's Disease

Takahiro Inoue, MD, Hideki Iijima, MD, PhD,* Michiko Tajiri, BS,† Shinichiro Shinzaki, MD, PhD,* Eri Shiraishi, MD,* Satoshi Hiyama, MD,* Akira Mukai, MD,* Sachiko Nakajima, MD, PhD,* Hirotsugu Iwatani, MD, PhD,‡ Tsutomu Nishida, MD, PhD,* Tsunekazu Mizushima, MD, PhD,§ Teruhito Yasui, PhD,‖,¶ Yoshitaka Isaka, MD, PhD,‡ Tatsuya Kanto, MD, PhD,*** Masahiko Tsujii, MD, PhD,* Eiji Miyoshi, MD, PhD,†† Yoshinao Wada, MD, PhD,† and Tetsuo Takehara, MD, PhD**

Background: Ideal biomarkers are required to be developed for the diagnosis and prediction of the treatment of inflammatory bowel disease (IBD). We have reported that alteration of *N*-linked oligosaccharides of immunoglobulin (Ig) G is a novel diagnostic marker of IBD. Oligosaccharide alterations of IgA, however, have not been investigated in IBD patients.

Methods: *N*- and *O*-linked oligosaccharides of serum IgA purified from 32 patients with Crohn's disease (CD), 30 patients with ulcerative colitis (UC), and 30 healthy volunteers (HV) were analyzed with high-performance liquid chromatography and mass spectrometry. Enzymes related to oligosaccharide attachment were investigated.

Results: *N*-linked oligosaccharides of IgA were not different between IBD and HV. In contrast, the number of *N*-acetylgalactosamines per hinge glycopeptide (GalNAc/HP) in the *O*-linked oligosaccharides of IgA was significantly decreased in patients with CD compared with UC and HV. GalNAc/HP had high sensitivity and specificity for discriminating between CD and HV based on receiver operating characteristic analysis. Lower GalNAc/HP was associated with more severe disease activity of CD. Changes in GalNAc/HP levels in 6 weeks after treatment with infliximab were associated with the clinical activity of CD at 30 weeks. GalNAc transferase expression of naïve B cells and extent of GalNAc attachment in IgA were significantly decreased by interleukin-21 in vitro.

Conclusions: The number of GalNAc attached in the IgA *O*-linked glycans of CD patients was significantly decreased, and strongly correlated with the clinical activity. Alterations of GalNAc attachment in IgA could be useful as a novel diagnostic and prognostic marker of CD.

(Inflamm Bowel Dis 2012;18:1723–1734)

Key Words: inflammatory bowel diseases, Crohn's disease, *O*-linked oligosaccharide, IgA, biomarker

Additional Supporting Information may be found in the online version of this article.

Received for publication December 12, 2011; Accepted December 19, 2011.

From the *Department of Gastroenterology and Hepatology, Osaka University Graduate School of Medicine, Suita, Osaka, Japan, †Research Institute, Osaka Medical Center and Research Institute for Maternal and Child Health, Izumi, Osaka, Japan, ‡Department of Geriatric Medicine and Nephrology, Osaka University Graduate School of Medicine, Suita, Osaka, Japan, §Department of Gastroenterological Surgery, Osaka University Graduate School of Medicine, Suita, Osaka, Japan, ‖Department of Molecular Immunology, Immunology Frontier Research Center, Osaka University, Suita, Osaka, Japan, ¶Department of Molecular Immunology, Research Institute for Microbial Diseases, Osaka University, Suita, Osaka, Japan, **Department of Dendritic Cell Biology and Clinical Application, Osaka University Graduate School of Medicine, Suita, Osaka, Japan, ††Department of Molecular Biochemistry and Clinical Investigation, Osaka University Graduate School of Medicine, Suita, Osaka, Japan.

Reprints: Tetsuo Takehara, MD, PhD, Department of Gastroenterology and Hepatology, Osaka University Graduate School of Medicine, 2-2 K1 Yamadaoka, Suita, Osaka 565-0871, Japan (e-mail: takehara@gh.med.osaka-u.ac.jp).

DOI 10.1002/ibd.22876

Published online 12 January 2012 in Wiley Online Library (wileyonlinelibrary.com).

Inflammatory bowel diseases (IBDs) are chronic intestinal disorders comprised of two major types: Crohn's disease (CD) and ulcerative colitis (UC). Although their pathophysiology remains unclear, recent studies have suggested that IBD is induced by a failure of the homeostatic mechanism of intestinal mucosal immune responses.[1–3] To date, there are no serologic markers with sensitivity and specificity high enough to diagnose IBD.[4] In addition, there are no ideal serologic markers to predict the clinical course of IBD. Thus, noninvasive serological markers of IBD must be developed in order to diagnose IBD and to predict responders to treatments. We have recently shown that oligosaccharide alterations in the *N*-glycan of serum immunoglobulin (Ig) G can be a novel diagnostic marker of IBD.[5]

In the mucosal immune system, IgA rather than IgG acts as the first line of defense against antigens or pathogens in the gut.[6] Dysregulation of IgA-mediated homeostasis is suggested to trigger inflammatory disorders, such as

TABLE 1. Patient Characteristics

	HV (n = 30)	DC (n = 17)	UC (n = 30)	CD (n = 32)	IgAN (n = 10)
Male/female	13/17	9/8	15/15	24/8	4/6
Age, y	37 ± 9	39 ± 16	41 ± 14	36 ± 12	32 ± 7
Age at diagnosis, y			35 ± 13	27 ± 9	
Bowel surgery, n (%)			0 (0)	19 (59)	
Extraintestinal manifestations, n (%)			0 (0)	3 (9)	
Treatment					
Salazosulfapyridine or mesalazine, n (%)			27 (90)	29 (91)	
Corticosteroids, n (%)			6 (20)	3 (9)	
Immunomodulators, n (%)			0 (0)	3 (9)	
Infliximab, n (%)			0 (0)	0 (0)	
Total parental nutrition or elemental diet, n (%)			2 (7)	13 (41)	
Disease location					
Small bowel/colon/small bowel and colon				11/5/16	
Total /left colon/rectum and sigmoid			13/10/7		
Disease behavior of CD					
Inflammatory/stricturing/penetrating/unknown				11/8/10/3	
Disease severity of UC					
Clinical remission/mild/moderate/severe			4/15/9/2		
CRP, mg/dL		7.7 ± 7.8	1.1 ± 3.3	1.1 ± 2.1	
CAI (UC) or CDAI (CD)			13 ± 7	184 ± 89	

IgAN, IgA nephropathy. The data are expressed as the mean ± SD in age, age at diagnosis, CRP, CAI, and CDAI. Other categories are shown as n (%).

IBD and celiac disease.[7] IgA contains N-linked carbohydrates at position 263 in the constant region of heavy chain (C_H) 2 and at position 459 in the tail-piece extension of C_H3. IgA_2 contains additional N-glycans in C_H1 and C_H2.[8] In addition to the N-glycosylation sites, IgA_1 has nine potential O-glycosylation sites in the 23-amino acid, proline-rich hinge region and usually four or five O-glycosylation sites are occupied by oligosaccharides.[9] IgA_2 lacks this hinge region and is not O-glycosylated. The mucin-type O-glycosylation is initiated by linking N-acetylgalactosamine (GalNAc) to the Ser or Thr of the protein backbone and this reaction is catalyzed by GalNAc transferases.[10,11] Oligosaccharide alterations of IgA related to disease have been studied in considerable detail in IgA nephropathy, in which IgA antibodies with agalactosyl O-linked oligosaccharides are precipitated in the nephron.[12] Oligosaccharide alterations of IgA, however, have not been investigated in IBD.

Recently, mass spectrometry (MS) has been shown to be an effective tool for quantitation and measurement of site-occupancy of O-glycans.[13] In this study we performed a detailed oligosaccharide analysis of N- and O-linked IgA glycans in IBD patients. We found that the number of N-acetylgalactosamines per hinge glycopeptide (GalNAc/HP) attached in the IgA O-linked glycopeptides of IBD patients was significantly decreased in patients with CD compared with healthy volunteers (HV). GalNAc/HP significantly negatively correlated with the Crohn's Disease Activity Index (CDAI) in CD. The enzymes related to the reduction of GalNAc/HP were further analyzed.

MATERIALS AND METHODS

Subjects

Serum samples were collected from 32 patients with CD, 30 patients with UC, 30 HV, 17 patients with colonic inflammation including appendicitis, diverticulitis, and ischemic colitis (disease control; DC), and 10 patients with IgA nephropathy (Table 1). Intestinal tissues from patients with CD and HV were obtained during colonoscopy and surgery. All patients were Japanese and were recruited at the Department of Gastroenterology and Hepatology or Department of Geriatric Medicine and Nephrology, Osaka University Hospital (Suita, Osaka, Japan). Patients were diagnosed with CD or UC according to endoscopic, radiologic, histologic, and clinical criteria provided by the Council for International Organizations of Medical Sciences in the World Health Organization and the International Organization for the Study of Inflammatory Bowel Disease.[14,15] Disease behavior in CD (B1: nonstricturing and nonpenetrating; B2: stricturing; B3: penetrating) and disease severity in UC (S0: clinical remission; S1: mild; S2: moderate; S3: severe) were determined based on the Montreal Classification.[16] Clinical activity was determined

using the CDAI for CD[17] or the Clinical Activity Index (CAI) for UC.[18] IgA nephropathy was diagnosed histologically by renal biopsy. Detailed patient characteristics are presented in Table 1. Oligosaccharides of serum samples were measured before and after treatment with infliximab in 10 consecutive CD patients.

Analysis of *N*-linked Oligosaccharide of IgA by Reverse Phase High-performance Liquid Chromatography (HPLC)

IgA_1 samples were isolated from 200 μL of serum using jacalin affinity chromatography (Vector Laboratories, Burlingame, CA).[19] *N*-linked oligosaccharides were released from serum IgA_1 and labeled with 2-aminopyridine, as described previously.[20] Briefly, *N*-linked oligosaccharides were released from purified IgA_1 samples by overnight incubation with 0.5 mU glycopeptidase F (Takara Bio, Shiga, Japan). Oligosaccharides were labeled with 2-aminopyridine by GlycoTag (Takara Bio) and incubated with 2 M acetic acid to remove sialic acids. Pyridylamino-oligosaccharides from IgA_1 were analyzed on a reverse phase HPLC system (Waters, Milford, MA). Pyridylamino-oligosaccharides were detected using a fluorescence detector (Waters 2475) at wavelengths of 320 nm for excitation and 400 nm for emission.

Analysis of *O*-Linked Oligosaccharide of IgA Hinge Glycopeptides by Matrix-Assisted Laser Desorption Ionization Time-of-Flight Mass Spectrometry (MALDI-TOF MS)

IgA samples from 20 μL of serum were purified using affinity chromatography, which was manufactured by coupling anti-IgA antibody (Dako, Glostrup, Denmark) to a HiTrap NHS-activated HP column (GE Healthcare, Fairfield, CT). Isolated IgA was dissolved in a 0.5 mL solution of 6 M guanidine, 0.25 M Tris-HCl, pH 8.0, and then S-carbamidomethylated with 0.22 M iodoacetamide for 30 minutes at room temperature. After reaction, these chemicals were removed by gel filtration using an NAP5 column (GE Healthcare), and lysyl endopeptidase (Wako Pure Chemical Industries, Osaka, Japan) and trypsin (Promega, Fitchburg, WI) were added to the solution, which was then incubated at 37°C for 6 hours. Enrichment of glycopeptides from digests was carried out according to a method described previously.[21] Briefly, a typical 100-μg digest was mixed with a 15-μL packed volume of Sepharose CL4B in butanol/ethanol/H_2O (4:1:1, v/v). The gel was then incubated with an aqueous solvent of ethanol/H_2O (1:1 v/v) for 30 minutes and the solution phase was recovered and dried using a vacuum concentrator. Desialylation of glycopeptides was carried out by incubation in 2 M acetic acid at 80°C for 2 hours. MALDI-TOF-MS was carried out on a Voyager DE Pro MALDI-TOF mass spectrometer with a nitrogen pulsed laser (Applied Biosystems, Foster City, CA). The peptide sample was mixed with 10 mg/mL of 2,5-dihydroxybenzoic acid dissolved in a 0.1% (v/v) trifluoroacetic acid and 50% (v/v) acetonitrile solution for measurement. The measurements were carried out in positive ion and linear TOF mode. The mass spectra acquired by at least 200 laser shots were accumulated and the measurement was repeated at least three times.[22] The molar content of the component saccharides, GalNAc/HP and galactose per hinge glycopeptides (Gal/HP), was calculated by Equation 1 followed by Equation 2. Equation 1: (Glyco) peptide Peak % = [(Glyco) peptide Peak Intensity] / [Total (Glyco) peptide Intensity] $\times$ 10^{-2}. Equation 2: GalNAc/HP, Gal/HP (mol/hinge glycopeptide) = Σ {(Glycopeptide Peak %) $\times$ (Number of GalNAc or Gal in the Glycopeptide)} $\times$ 10^{-2}.[13] The MALDI-TOF MS analysis was reproducible in repeated analysis of the same sample and we usually analyzed the oligosaccharides once per one sample.

Analysis of Anti-*Saccharomyces cerevisiae* Antibody (ASCA)

Serum ASCA concentrations were examined using the ASCA IgG enzyme-linked immunosorbent assay kit (Genesis Diagnostics, Cambridge, UK) according to the manufacturer's instructions. Values over 10 U/mL were defined as positive.

Isolation of B Cells and Naïve B Cells from Peripheral Blood Mononuclear Cells

Peripheral blood mononuclear cells were isolated from the heparinized venous blood of subjects by Ficoll–Hypaque density-gradient centrifugation. B cells and naïve B cells were separated by a B-cell isolation kit II and anti-IgD microbeads, respectively (Miltenyi Biotech, Bergisch Gladbach, Germany). Naïve B cells were cultured for 5 days in the presence of cytokines that induce IgA maturation; recombinant human CD40L (200 ng/mL; R&D Systems, Minneapolis, MN), interleukin (IL)-21 (50 ng/mL; BioSource International, Camarillo, CA), IL-10 (50 ng/mL; BioSource), or a proliferation-inducing ligand (APRIL, 500 ng/mL; R&D Systems).

Real-time Reverse Transcription Polymerase Chain Reaction (RT-PCR) for GALNT2

Total cellular RNA was isolated using Isogen-LS (Wako), and complementary DNA was synthesized from 0.1 to 0.5 μg of total RNA using the High Capacity RNA-to-cDNA Kit (Applied Biosystems). For TaqMan real-time RT-PCR, the reaction mixture was prepared by TaqMan Universal PCR Master Mix with predesigned and prelabeled TaqMan PCR primer and probe set for human polypeptide *N*-acetylgalactosaminyltransferase 2 (GALNT2), human IgA heavy chain, or human beta-actin endogenous control (Applied Biosystems). Real-time PCR was performed using an ABI PRISM 7900HT Sequence Detection System instrument and software (Applied Biosystems). Each sample was run in duplicate. The relative amount of GALNT2 RNA was calculated with the $\Delta\Delta$Ct method[23] and normalized to IgA heavy chain.

Lectin Immunohistochemistry

Intestinal tissues from patients with CD and HV were embedded in paraffin. Tissue sections (5 μm thick) were

deparaffinized, rehydrated, and subjected to antigen retrieval by incubation in a pressurized heating chamber (Dako). The sections were incubated in FITC-labeled mouse anti-human IgA_1 or IgA_2 (Southern Biotech, Birmingham, AL) and biotinylated jacalin (Vector Laboratories) followed by Texas red streptavidin (Vector Laboratories). The sections were mounted with Vectashield Hard Set Mounting Medium with DAPI (Vector Laboratories) and subjected to examination with a fluorescent microscope (Keyence BZ9000, Osaka, Japan).

Statistical Analysis

Differences were tested with the Mann–Whitney *U*-test or the Kruskal–Wallis test followed by the Mann–Whitney *U*-test, where appropriate. Either the $\chi 2$ test, $\chi 2$ test with Yates' correction (when sample number was less than 10), or Fisher's exact test (when sample number was less than 4), where appropriate, was used for the comparison of frequencies. Sensitivity for each test result was defined as the probability of a positive test result in a patient with the disease under investigation. Specificity was defined as the probability of a negative test result in a patient without the disease under investigation. A receiver operating characteristic (ROC) curve was generated by plotting sensitivity versus 1-specificity.[24,25] Area under the curve (AUC) was calculated by JMP software (SAS Institute, Cary, NC). $P < 0.05$ was considered statistically significant.

Ethical Considerations

This study protocol was approved by the ethical committee of Osaka University Graduate School of Medicine and written informed consent was obtained from each participant.

RESULTS

N-linked Oligosaccharide Analysis of IgA in IBD Patients

We previously demonstrated that *N*-linked oligosaccharide structures of IBD patients are significantly different from those of healthy subjects.[5] Terminal galactoses of *N*-linked oligosaccharides in serum IgG are highly depleted in patients with IBD. We first analyzed *N*-linked oligosaccharide structures of IgA_1 using HPLC. The agalactosyl peaks of fucosylated *N*-linked oligosaccharides (G0F) of IgA_1 were low and were similar between HV and CD (Fig. 1A). In addition, the galactosyl peaks of fucosylated *N*-linked oligosaccharides (G2F) of IgA_1 were also similar between HV and CD (Fig. 1A). When the peak height ratios of G0F/G2F of *N*-linked oligosaccharides of IgA_1 were calculated, they were not significantly different between CD, UC, and HV (data not shown), whereas the peak height ratios of G0F/G2F were increased in IgG samples of CD and UC compared with HV (Fig. 1B). These findings indicate that the levels of *N*-linked agalactosyl IgA oligosaccharides are not different between IBD and HV.

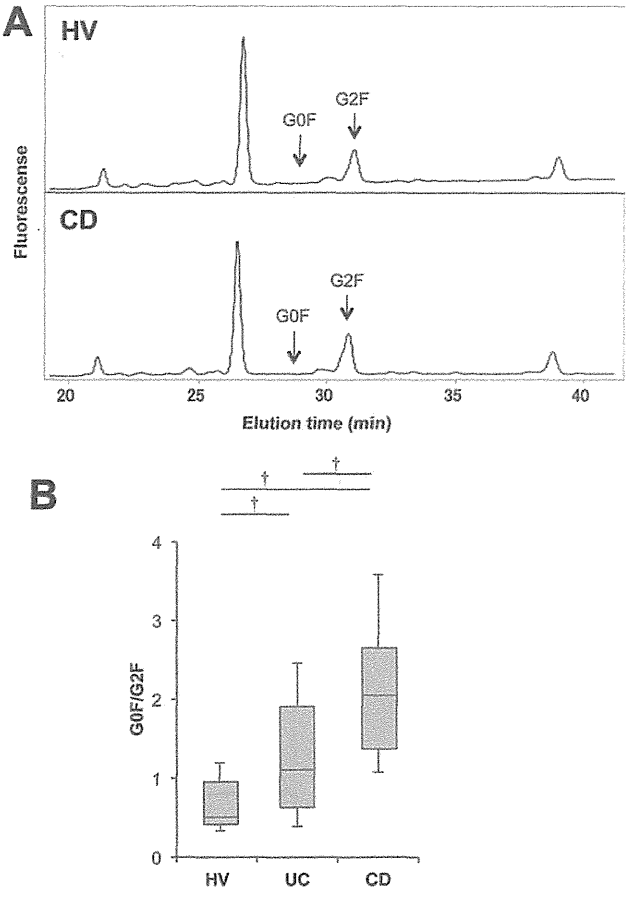

FIGURE 1. Analysis of *N*-linked oligosaccharides of immunoglobulins purified from HV and IBD patients. (A) Representative profiles of *N*-linked IgA_1 oligosaccharides of HV and CD patient. IgA was purified from the sera of HV and CD patients using jacalin affinity chromatography and the structures of IgA_1 *N*-linked oligosaccharides were analyzed by HPLC. G0F, the agalactosyl peak of fucosylated *N*-linked oligosaccharides; G2F, the galactosyl peaks of fucosylated *N*-linked oligosaccharides. (B) The ratio of agalactosyl/galactosyl fraction of fucosylated oligosaccharides (G0F/G2F) in the *N*-linked oligosaccharides of IgG. Boxplots show 50% of the relevant patient population. The line inside the box represents median value. Whiskers indicate the 90th and 10th percentiles. †$P < 0.05$.

Number of *N*-acetylgalactosamines in the *O*-linked Oligosaccharides of IgA Is Decreased in CD Patients

We next analyzed the *O*-linked oligosaccharides of IgA_1. Because complex *O*-linked oligosaccharide structures are difficult to analyze by HPLC, we used MALDI-TOF MS for the detailed analysis of *O*-linked oligosaccharide structures of IgA_1. Each peak of MALDI-TOF MS chart has been shown to correspond with each oligosaccharide attached in the IgA HP.[13] The MALDI-TOF MS analysis revealed that the peaks corresponding to the five or six GalNAc sugar residues of CD patients were lower than those of HV (Fig. 2A). In contrast, the peaks corresponding to the three or four GalNAc sugar residues of CD patients

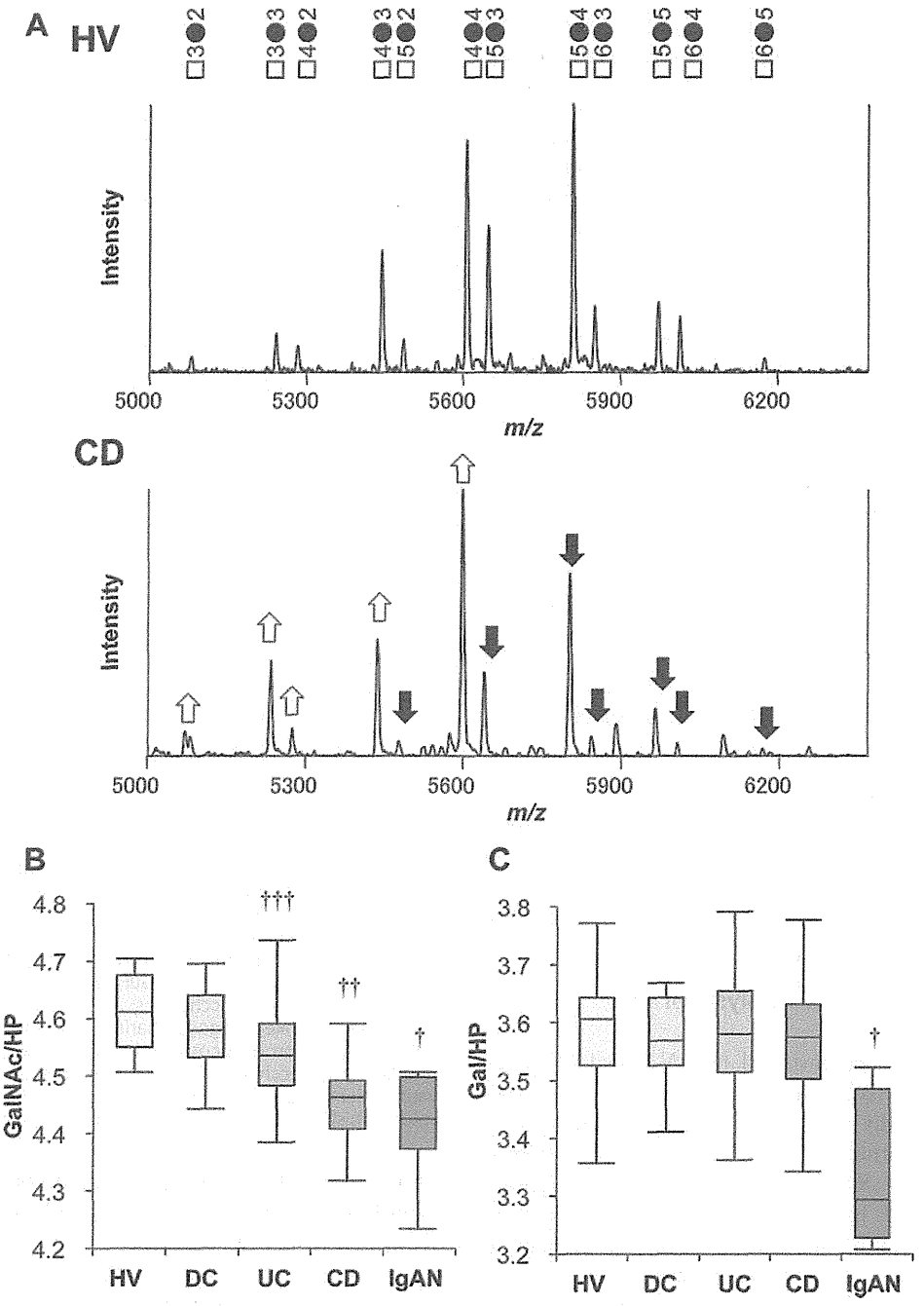

FIGURE 2. Analysis of *O*-linked oligosaccharides in hinge glycopeptides of IgA. Hinge glycopeptides that contain *O*-linked oligosaccharides were isolated and analyzed by MALDI-TOF mass spectrometry. Mass spectra of 30 HV, 17 patients with DC, 30 patients with UC, 32 patients with CD, and 10 patients with IgAN were evaluated. (A) Representative charts of MALDI-TOF mass spectra of *O*-linked oligosaccharides in IgA_1 hinge glycopeptides of HV and CD. IgA was purified from the sera using IgA affinity chromatography and hinge glycopeptides that contain *O*-linked oligosaccharides were isolated. □, GalNAc; ●, Gal; and □4●3 represents 4 GalNAc and 3 Gal attached to the hinge glycopeptide of IgA. The peaks corresponding to the five or six GalNAc sugar residues of CD patients (closed arrows) were lower than those of HV. In contrast, the peaks corresponding to the three or four GalNAc sugar residues of CD patients (open arrows) were higher than those of HV. (B) The number of GalNAc per hinge glycopeptide (GalNAc/HP) was analyzed using MALDI-TOF mass spectra. (C) The number of galactose residues per hinge glycopeptide (Gal/HP) was analyzed. DC, disease control; IgAN, IgA nephropathy. Boxplots show 50% of the relevant patient population. The line inside the box represents median value. Whiskers indicate the 90th and 10th percentiles. †$P < 0.05$ to HC, DC, UC, and CD; ††$P < 0.05$ to HV, DC, and UC; †††$P < 0.05$ to HV.

were higher than those of HV (Fig. 2A). Similar results were obtained when we analyzed several serum samples obtained from CD patients and HV. To confirm that GalNAc attachment in the hinge region of IgA is decreased in CD compared with HV, we next calculated the number of GalNAc attached to the IgA HP in patients with CD, UC, DC, IgA nephropathy, and HV. The number of GalNAc per each HP (GalNAc/HP) was significantly lower in patients with CD and IgA nephropathy than in patients with UC, DC, and HV (Fig. 2B). In addition, the number of GalNAc/HP was significantly lower in patients with UC compared with HV (Fig. 2B). The number of GalNAc/HP in UC, however, was not different from that in DC (Fig. 2B). We next calculated the mean number of galactose residues per each HP (Gal/HP). The number of Gal/HP residues was significantly decreased in patients with IgA nephropathy compared with HV (Fig. 2C), which was consistent with a previous report.[26] In contrast to the deficiency of GalNAc/HP in IBD patients, the Gal/HP levels were not significantly different between IBD patients and HV (Fig. 2C).

Decrease of GalNAc in IgA *O*-linked Oligosaccharides Is Associated with an Increase in CDAI

We then investigated the relationship between GalNAc/HP and the clinical activity of CD and UC. GalNAc/HP showed a significantly negative correlation with CDAI in CD (Fig. 3A). When the CD patients were divided into those with active disease (CDAI $\geq$150) and those in remission (CDAI $<$150), GalNAc/HP was significantly lower in the active patients than in the remissive patients (Fig. 3B). GalNAc/HP levels were significantly lower in patients with stricture or penetration (Montreal category: B2+B3) than those with no evidence of stricture or penetration (Montreal category: B1, Fig. 3C). GalNAc/HP also showed a significantly negative correlation with CAI in UC (Fig. 3D). GalNAc/HP in active UC patients (CAI $\geq$6), however, did not significantly differ from that in patients in remission (CAI $<$6, Fig. 3E). In addition, GalNAc/HP levels were not significantly different among the Montreal categories (Fig. 3F). These findings indicate that the decreased GalNAc levels in IgA *O*-linked oligosaccharides are associated with active disease status of CD.

GalNAc/HP as a New Serologic Marker for CD

We then investigated the effectiveness of the IgA *O*-linked oligosaccharide analysis as the serologic marker of IBD. In order to define the optimal cutoff value with the highest diagnostic accuracy, we performed multiple ROC curve analyses for distinct GalNAc/HP. The highest AUC was calculated for a GalNAc/HP of 4.50 with a sensitivity of 0.81 and specificity of 1.00. We defined GalNAc/HP $<$4.50 as "GalNAc deficient." The GalNAc deficient rate in CD, UC, HV, and DC was 81%, 30%, 0%, and 11%, respectively (Fig. 4A). We next compared the sensitivity and specificity of GalNAc/HP with those of ASCA for the discrimination of IBD using an ROC curve. Both the sensitivity and specificity of GalNAc/HP were higher than those of ASCA for differentiation of CD and HV (AUC of GalNAc/HP vs. ASCA; 0.94 vs. 0.75, Fig. 4B). Moreover, both the sensitivity and specificity of GalNAc/HP were higher than those of ASCA for the differentiation of CD and UC (AUC of GalNAc/HP vs. ASCA; 0.71 vs. 0.59, Fig. 4C).

Alteration of *O*-linked Oligosaccharides Is Detectable in Inflamed Mucosa of CD Patients

To investigate where GalNAc-deficient IgA is produced in IBD patients, we performed lectin immunohistochemistry by using jacalin (galactose-GalNAc binding lectin) of intestinal tissues obtained from the patients with CD and HV. The number of the cells costained with anti-IgA_1 antibody and jacalin in the lamina propria was lower in CD patients than in HV (Fig. 5). In contrast, lamina propria cells costained with anti-IgA_2 antibody and jacalin were not observed in either CD patients or HV (Supporting Fig. 1). These findings show GalNAc in *O*-linked IgA oligosaccharides is deficient in the mucosal IgA_1-producing cells of CD patients.

Expression of GalNAc Transferase mRNA Is Decreased in the Inflammatory Condition

In patients with IgA nephropathy, decreased activity of galactose transferase (C1GALT1; core 1 synthase, glycoprotein-*N*-acetylgalactosamine 3-beta-galactosyltransferase, 1) in B cells is responsible for the reduction of galactose in the IgA *O*-linked oligosaccharides.[27] We therefore investigated GalNAc transferase (GALNT2; polypeptide *N*-acetylgalactosaminyltransferase 2) expression, which may be responsible for the attachment of GalNAc in the peripheral blood B cells of the patients with CD. GALNT2 mRNA expression in the peripheral blood B cells and immortalized B cells by infection with Epstein–Barr virus isolated from IBD patients, however, was not decreased when compared with HV (data not shown). Because oligosaccharide alterations in IgA are suggested to take place in the inflamed mucosa, we next stimulated naïve B cells with CD40L, IL-21, and IL-10, all of which have been shown to provide signals for the maturation of IgA producing cells in the mucosa.[28,29] CD40L is essential for T-cell-dependent isotype switching of naïve B cells to IgA-producing cells, and both IL-10 and IL-21 can switch activated naïve B cells to IgA-producing plasma cells in the presence of CD40L. IL-21 is increased in the inflamed mucosa of the patients with CD.[30] When the naïve B cells were stimulated with CD40L and IL-21 in vitro, GALNT2 was

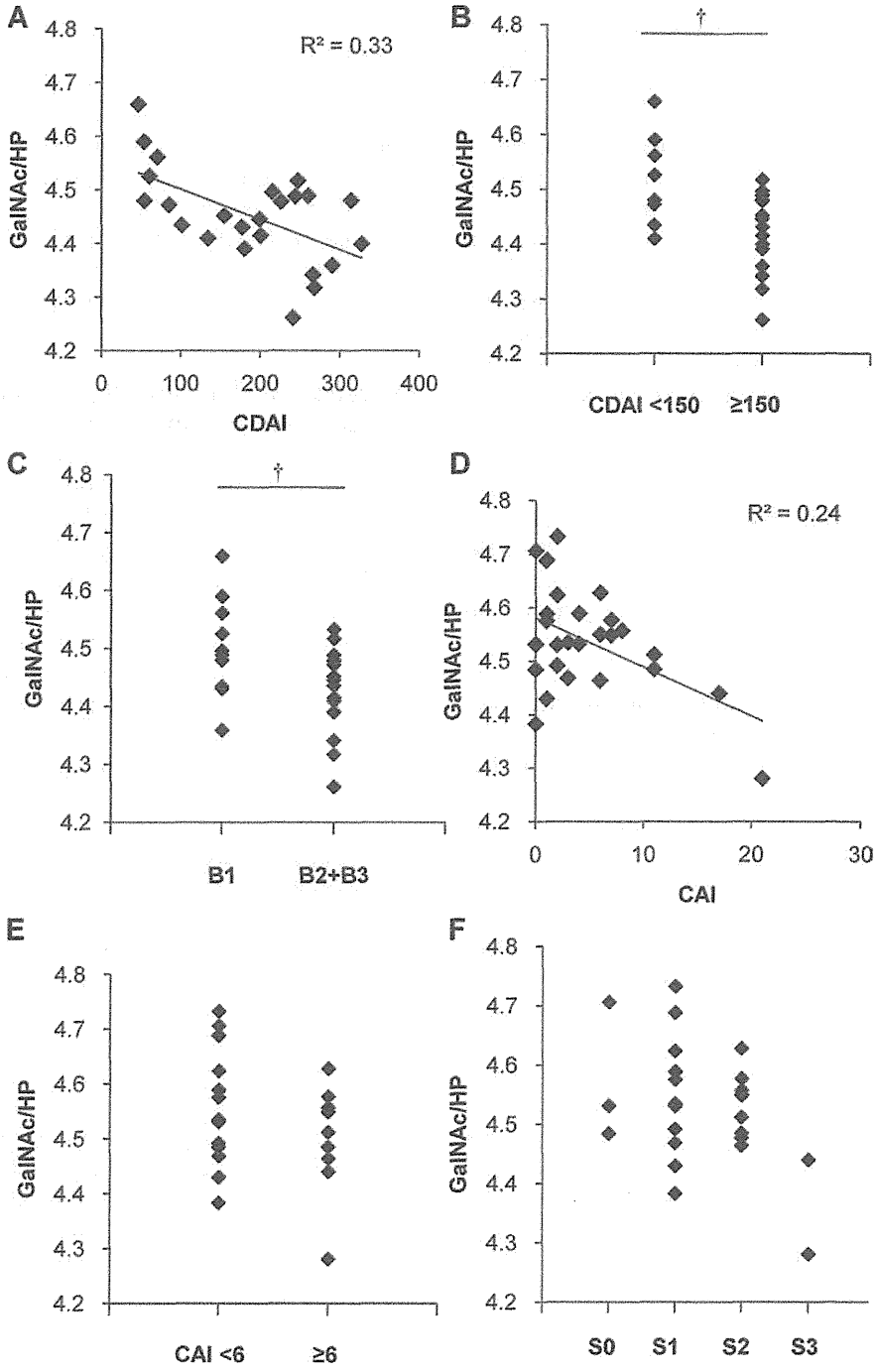

FIGURE 3. Relationship between GalNAc/HP and disease activity. (A) Relationship between GalNAc/HP and CDAI in CD. (B) GalNAc/HP of CD patients in remission (CDAI <150) and in an active stage (CDAI ≥150). (C) GalNAc/HP of CD patients with category B1 and B2+B3 in the Montreal Classification. (D) Relationship between GalNAc/HP and CAI in UC. (E) GalNAc/HP of UC patients in CAI <6 and in CAI ≥6. (F) GalNAc/HP of UC patients with category S0, S1, S2, S3, and S4 in the Montreal Classification. †$P < 0.05$.

significantly decreased when compared with CD40L alone or CD40L and IL-10 ($P < 0.05$; Fig. 6A). Consistent with the decrease in GALNT2, GalNAc/HP levels in the IgA *O*-linked oligosaccharides were lower in the presence of CD40L and IL-21 (GalNAc/HP, 4.37) than the presence of CD40L alone (GalNAc/HP, 4.47; Fig. 6B).

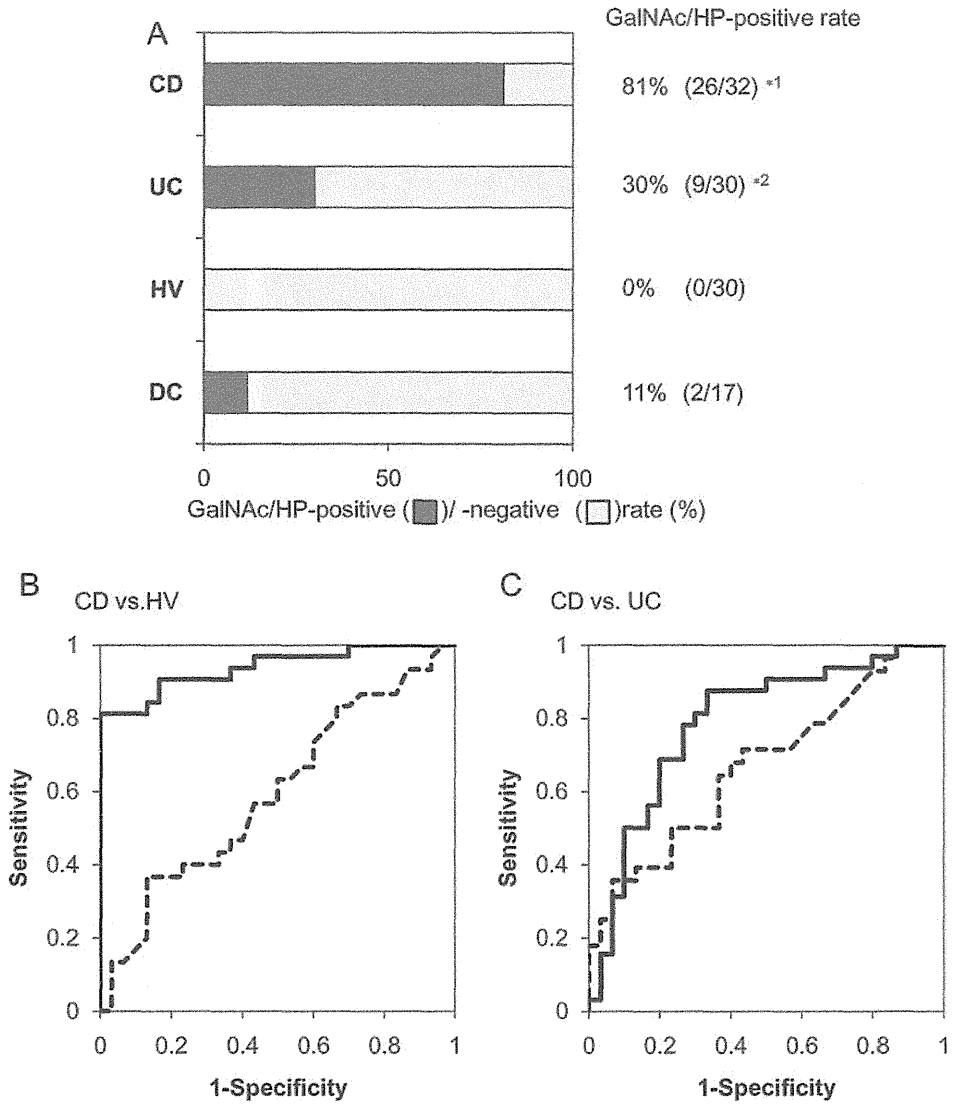

FIGURE 4. Effectiveness of GalNAc/HP-positive rate as a serologic marker for IBD. (A) GalNAc/HP-positive rates were analyzed in CD, UC, HV, and DC. The cutoff point of GalNAc deficient was determined 'GalNAc/HP = 4.50' by ROC curve. Fisher's exact test was used for the comparison between CD and UC, HV, or DC and between UC and HV. *1$P < 0.05$ to UC, HV, and DC. *2$P < 0.05$ to HV. (B) The ROC curves for GalNAc/HP (solid line) and ASCA (dotted line) levels for the discrimination between CD and HV, or (C) between CD and UC. Sensitivity is represented on the y-axis and 1-specificity on the x-axis.

Alteration of Oligosaccharides in IgA Recovers and Predicts Clinical Course After Treatment with Infliximab

We next investigated whether GalNAc/HP in IgA is affected by the treatment with infliximab, an antibody against tumor necrosis factor-alpha. When the levels of GalNAc/HP were compared between 0 and 6 weeks after the treatment with infliximab in 10 CD patients, GalNAc/HP was significantly higher at 6 weeks than 0 weeks ($P < 0.05$, Fig. 7A). In seven patients whose GalNAc/HP was increased at 6 weeks compared with that at 2 weeks, CDAI scores were decreased at 30 weeks compared with 0 weeks (Fig. 7B). In contrast, in three patients whose GalNAc/HP was decreased at 6 weeks compared with that at 2 weeks, CDAI scores were elevated after the treatment, including one patient who required small bowel resection (Fig. 7B).

DISCUSSION

We recently reported that terminal galactoses are highly depleted in the *N*-linked oligosaccharides of IgG in IBD patients when compared with healthy subjects.[5] IgA, rather than IgG, functions as a first line of defense in the mucosal immune system and functional abnormalities of IgA have been shown to cause mucosal immune disorders,

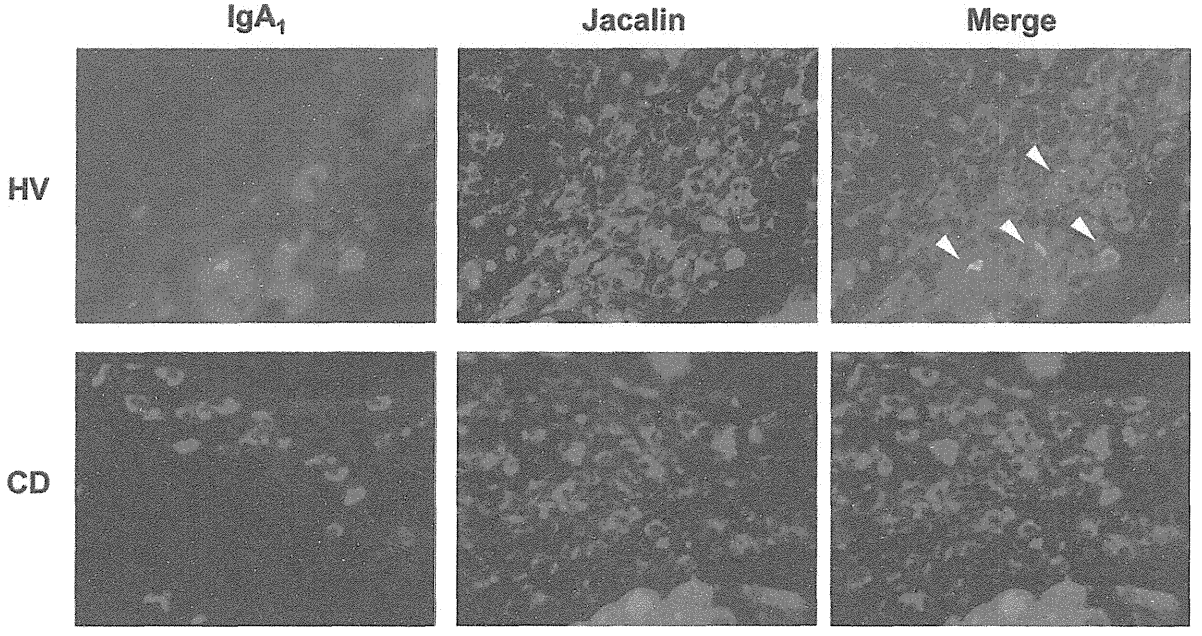

FIGURE 5. Alterations of IgA_1 *O*-linked oligosaccharides in the inflamed intestine of CD patients. Immunohistochemistry of the small intestine costained with anti-IgA_1 antibody and jacalin, a galactose-GalNAc-specific lectin. Tissue sections of the small intestine of HV and inflamed small intestine of CD were stained with anti-IgA_1-FITC antibody (green) and jacalin-Texas red (red). Double-positive cells for IgA_1 and jacalin were observed in the mucosa of HV (arrowhead), but were decreased in the inflamed mucosa of CD. Representative pictures are shown.

such as IBD; selective IgA deficiency is shown to be associated with development of IBD.[31,32] An association of linear IgA dermatosis and IBD has also been reported.[33] The association of IgA oligosaccharide alterations and IBD, however, has not yet been reported. We demonstrate for the first time that *O*-linked, but not *N*-linked, oligosaccharide structures of serum IgA_1 are significantly altered in patients with CD compared with healthy subjects. Alterations of *O*-linked oligosaccharides were not due to galactose-deficiency, but rather to GalNAc-deficiency. Galactose-deficiency of *N*-linked oligosaccharides in IgG and GalNAc-deficiency of *O*-linked oligosaccharides in IgA were also reported in patients with rheumatoid arthritis, which is a similar immunologic disorder as CD.[34] Our results suggest that CD has a biochemical disorder similar to rheumatoid arthritis for the formation of oligosaccharides of IgA and IgG. Association of *O*-linked oligosaccharides in IgA and disease development is best studied in detail in IgA nephropathy. Galactose-deficiency of *O*-linked oligosaccharides in IgA is commonly observed in patients with IgA nephropathy and can be a cause of nephron damage.[35,36] Indeed, IgA nephropathy is sometimes associated both with UC[37] and CD,[38] and IgA nephropathy followed after IBD is called secondary IgA-nephropathy.[39] The *O*-linked oligosaccharide structures of IBD patients, however, were different from those of IgA nephropathy in terms of galactose deficiency and none of the IBD patients in our cohort was suffering from IgA nephropathy. Thus, the mechanism and consequence of the alteration of *O*-linked oligosaccharides in IgA of IBD patients are different from those in patients with IgA nephropathy.

Among the several serologic markers reported to have diagnostic value for IBD, ASCA and perinuclear antineutrophil cytoplasmic antibody have been extensively investigated and shown to be effective for discriminating CD and UC, respectively.[40,41] More recently, additional serum antibodies have been reported in CD patients, including those against the Pseudomonas-associated sequence I2, outer membrane porin C of *Escherichia coli*, and against the bacterial flagellin cBir1.[42–44] Most recently, novel anti-glycan antibodies, such as against mannan (IgG anti-covalently attached anti-*Saccharomyces cerevisiae* antibodies) and anti-mannobioside (Man [a1,3]) carbohydrate IgG antibodies, were reported to link to CD.[45] These serologic markers carry high specificities comparable to ASCA, ranging from 80% to 90%.[46] Moreover, elevated levels of novel anti-glycan antibodies are associated with early disease onset, complicated disease behavior, and IBD-related surgery. On the other hand, the sensitivities of these markers, ranging from 20% to 55%, are not high enough for clinical use.[46] We demonstrated that GalNAc/HP, which has relatively high sensitivity and specificity for IBD, is a potential diagnostic marker for IBD. In addition, GalNAc/HP reflects the clinical activity of CD and can have a predictive value

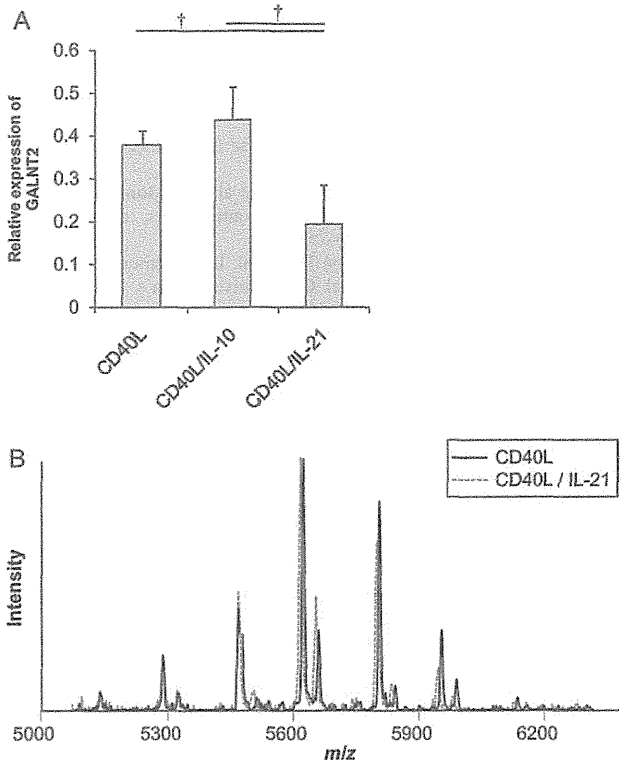

FIGURE 6. Reduction of GALNT2 expression and GalNAc of IgA O-linked oligosaccharides in B cells stimulated by IL-21. (A) The levels of polypeptide GalNAc transferase 2 (GALNT2) mRNA expression in B cells stimulated by cytokines that develop IgA-producing cells (CD40L, CD40L/IL-10, and CD40L/IL-21 [n = 4-9]). Results are shown as mean ± SE. †$P < 0.05$. (B) A representative chart of MALDI-TOF mass spectra of IgA O-linked oligosaccharides purified from B cells stimulated with CD40L (solid black spectrum) and CD40L/IL-21 (dotted red spectrum).

for treatment. Further studies are required regarding the efficacy of GalNAc/HP for the diagnosis and prediction in IBD patients using larger samples and a high-throughput screening system needs to be established.

We have shown that GalNAc attachment in IgA hinge region was decreased in CD. Since galactose-deficiency has been reported to be caused by systemic deficiency of galactosyltransferase in IgA nephropathy,[47] we speculated that GalNAc deficiency was due to the defect of GalNAc transferase activity in IBD patients. When freshly isolated peripheral blood B cells and IgA-producing cell lines obtained from IBD patients were analyzed, GalNAc transferase activity of IBD patients, however, was not decreased compared with that of HV. Lectin immunohistochemistry of the small intestine revealed that GalNAc-positive cells were rarely detectable in IgA_1-producing cells in the lamina propria of CD patients. Thus, a great difference was observed in the affinity to jacalin of IgA_1-producing cells between the inflamed mucosa of CD and normal mucosa of HV. The difference in the amount of GalNAc attached to serum IgA_1 between CD and HV, however, was relatively small. The affinity to jacalin on IgA_1-producing cells in noninflamed tissue of CD was high similarly to HV (data not shown). It is speculated that small changes in the serum IgA_1 oligosaccharides in CD may be due to the dilution of highly GalNAc-deficient oligosaccharides produced in inflammatory tissue with oligosaccharides in noninflamed tissue, which are similar to those of HV. To investigate the mechanisms of GalNAc-deficiency in the inflamed lesion of CD, we evaluated GALNT2 expression in IgA-producing cells stimulated with inflammatory cytokines related to the maturation of IgA-producing cells. We showed that GALNT2 expression was significantly lower in B cells stimulated by CD40L and IL-21 than by CD40L alone or CD40L and IL-10. In addition, GalNAc attachment was less in B cells stimulated with CD40L and IL-21 than CD40L alone. It has been reported that isotype switching from naïve B cells to IgA plasma cells can be induced by CD40L together with IL-10 and/or IL-21, and it is called the "T-cell-dependent pathway".[29] Likewise, APRIL and BAFF (B-cell-activating factor belonging to the tumor necrosis factor family) have also been reported to induce isotype switching to IgA in a T-cell-independent manner.[28] IL-21 is a cytokine that strongly induces IgA production,[29] and elevated IL-21 levels in the mucosa and elevated IL-21 receptor expression are observed in IBD patients.[30] Although IL-10 induces IgA production similarly to IL-21, production of IL-10 is decreased in CD patients.[48,49] When we cultured naïve B cells with APRIL, APRIL did not affect GALNT2 expression in vitro (data not shown). These results suggested that exposure to IL-21 in the mucosa of IBD can be one of the mechanisms for the defective GalNAc attachment in IgA and GalNAc/HP

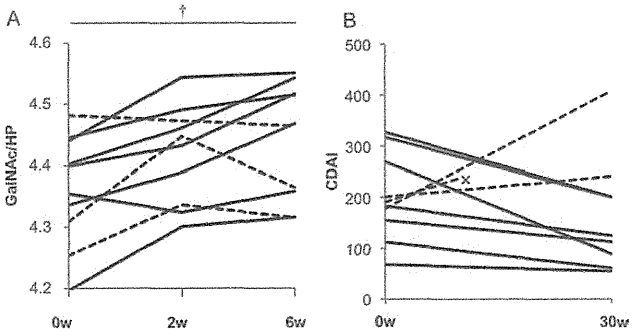

FIGURE 7. Alterations of O-linked oligosaccharides after treatment of infliximab. (A) GalNAc/HP levels before and after the treatment of infliximab. Ten patients with CD were treated with infliximab and serum samples were collected at 0 (before infliximab), 2, and 6 weeks. GalNAc/HP levels at 6 weeks were significantly higher than those at 0 weeks (†$P < 0.05$). (B) CDAI scores of CD patients from 0 and 30 weeks after treatment with infliximab. Three patients with decreased GalNAc/HP levels at 6 weeks compared with that at 2 weeks are indicated as dotted lines in (A,B). Cross mark shows that the patient received bowel surgery at 9 weeks.

might be recovered after the introduction of infliximab by the restoration of the mucosal cytokine network.

To date, it is unknown if the function of IgA with GalNAc deficiency is altered in IBD patients. It has been reported that *O*-linked oligosaccharides strengthen the attachment of IgA and bacteria as well as the binding of IgA and mannan binding lectin, which is associated with complement activation.[9] It has also been reported that T cells express receptors that have binding affinity with IgA *O*-linked oligosaccharides.[50] These reports suggest that oligosaccharide alterations of IgA possibly serve to modify the immune function of CD. Further studies are needed to investigate the function of IgA with altered *O*-linked oligosaccharides and these projects are ongoing in our laboratory.

In summary, GalNAc/HP in *O*-linked oligosaccharides of IgA is significantly decreased in CD patients and reflects disease activity and clinical course. These findings suggest that GalNAc/HP can be a novel serologic marker for CD, and thus be of predictive value of CD treatments.

ACKNOWLEDGMENT

We thank Dr. Jan Novak, Department of Microbiology, University of Alabama at Birmingham for providing the polymeric and monomeric IgA_1 myeloma protein that is deficient in galactose in *O*-linked glycans.

REFERENCES

1. Himmel ME, Hardenberg G, Piccirillo CA, et al. The role of T-regulatory cells and Toll-like receptors in the pathogenesis of human inflammatory bowel disease. *Immunology*. 2008;125:145–153.
2. Van Limbergen J, Russell RK, Nimmo ER, et al. Genetics of the innate immune response in inflammatory bowel disease. *Inflamm Bowel Dis*. 2007;13:338–355.
3. Kraus TA, Toy L, Chan L, et al. Failure to induce oral tolerance to a soluble protein in patients with inflammatory bowel disease. *Gastroenterology*. 2004;126:1771–1778.
4. Nikolaus S, Schreiber S. Diagnostics of inflammatory bowel disease. *Gastroenterology*. 2007;133:1670–1689.
5. Shinzaki S, Iijima H, Nakagawa T, et al. IgG oligosaccharide alterations are a novel diagnostic marker for disease activity and the clinical course of inflammatory bowel disease. *Am J Gastroenterol*. 2008;103:1173–1181.
6. Fagarasan S, Honjo T. Intestinal IgA synthesis: regulation of front-line body defences. *Nat Rev Immunol*. 2003;3:63–72.
7. Cerutti A, Rescigno M. The biology of intestinal immunoglobulin A responses. *Immunity*. 2008;28:740–750.
8. Yoo EM, Morrison SL. IgA: an immune glycoprotein. *Clin Immunol*. 2005;116:3–10.
9. Royle L, Roos A, Harvey DJ, et al. Secretory IgA N- and O-glycans provide a link between the innate and adaptive immune systems. *J Biol Chem*. 2003;278:20140–20153.
10. Tian E, Ten Hagen KG. Recent insights into the biological roles of mucin-type O-glycosylation. *Glycoconj J*. 2009;26:325–334.
11. Ten Hagen KG, Fritz TA, Tabak LA. All in the family: the UDP-GalNAc:polypeptide N-acetylgalactosaminyltransferases. *Glycobiology*. 2003;13:1R–16R.
12. Novak J, Julian BA, Tomana M, et al. IgA glycosylation and IgA immune complexes in the pathogenesis of IgA nephropathy. *Semin Nephrol*. 2008;28:78–87.
13. Wada Y, Tajiri M, Ohshima S. Quantitation of saccharide compositions of O-glycans by mass spectrometry of glycopeptides and its application to rheumatoid arthritis. *J Proteome Res*. 2010;9:1367–1373.
14. Podolsky DK. Inflammatory bowel disease (1). *N Engl J Med*. 1991;325:928–937.
15. Podolsky DK. Inflammatory bowel disease (2). *N Engl J Med*. 1991;325:1008–1016.
16. Satsangi J, Silverberg MS, Vermeire S, et al. The Montreal classification of inflammatory bowel disease: controversies, consensus, and implications. *Gut*. 2006;55:749–753.
17. Best WR, Becktel JM, Singleton JW, et al. Development of a Crohn's disease activity index. National Cooperative Crohn's Disease Study. *Gastroenterology*. 1976;70:439–444.
18. Rachmilewitz D. Coated mesalazine (5-aminosalicylic acid) versus sulphasalazine in the treatment of active ulcerative colitis: a randomised trial. *BMJ*. 1989;298:82–86.
19. Pack TD. Purification of human IgA. *Curr Protoc Immunol*. 2001; Chapter 2:Unit 2.10B.
20. Kondo A, Hosokawa Y, Kiso M, et al. Analysis of oligosaccharides of human IgG from serum of leukemia patients. *Biochem Mol Biol Int*. 1994;32:897–902.
21. Wada Y, Tajiri M, Yoshida S. Hydrophilic affinity isolation and MALDI multiple-stage tandem mass spectrometry of glycopeptides for glycoproteomics. *Anal Chem*. 2004;76:6560–6565.
22. Wada Y, Azadi P, Costello CE, et al. Comparison of the methods for profiling glycoprotein glycans—HUPO Human Disease Glycomics/Proteome Initiative multi-institutional study. *Glycobiology*. 2007;17:411–422.
23. Mullen AC, Hutchins AS, High FA, et al. Hlx is induced by and genetically interacts with T-bet to promote heritable T(H)1 gene induction. *Nat Immunol*. 2002;3:652–658.
24. Beck JR, Shultz EK. The use of relative operating characteristic (ROC) curves in test performance evaluation. *Arch Pathol Lab Med*. 1986;110:13–20.
25. Zweig MH, Campbell G. Receiver-operating characteristic (ROC) plots: a fundamental evaluation tool in clinical medicine. *Clin Chem*. 1993;39:561–577.
26. Hiki Y, Odani H, Takahashi M, et al. Mass spectrometry proves under-O-glycosylation of glomerular IgA1 in IgA nephropathy. *Kidney Int*. 2001;59:1077–1085.
27. Allen AC, Topham PS, Harper SJ, et al. Leucocyte beta 1,3 galactosyltransferase activity in IgA nephropathy. *Nephrol Dial Transplant*. 1997;12:701–706.
28. Litinskiy MB, Nardelli B, Hilbert DM, et al. DCs induce CD40-independent immunoglobulin class switching through BLyS and APRIL. *Nat Immunol*. 2002;3:822–829.
29. Avery DT, Bryant VL, Ma CS, et al. IL-21-induced isotype switching to IgG and IgA by human naive B cells is differentially regulated by IL-4. *J Immunol*. 2008;181:1767–1779.
30. Liu Z, Yang L, Cui Y, et al. Il-21 enhances NK cell activation and cytolytic activity and induces Th17 cell differentiation in inflammatory bowel disease. *Inflamm Bowel Dis*. 2009;15:1133–1144.
31. Hodgson HJ, Jewell DP. Selective IgA deficiency and Crohn's disease: report of two cases. *Gut*. 1977;18:644–646.
32. Yel L. Selective IgA deficiency. *J Clin Immunol*. 2010;30:10–16.
33. Barberis C, Doutre MS, Bioulac-Sage P, et al. [Linear IgA bullous dermatosis associated with Crohn's disease.] *Gastroenterol Clin Biol*. 1988;12:76–77.
34. Field MC, Amatayakul-Chantler S, Rademacher TW, et al. Structural analysis of the N-glycans from human immunoglobulin A1: comparison of normal human serum immunoglobulin A1 with that isolated from patients with rheumatoid arthritis. *Biochem J*. 1994;299(Pt 1):261–275.
35. Tomana M, Novak J, Julian BA, et al. Circulating immune complexes in IgA nephropathy consist of IgA1 with galactose-deficient hinge region and antiglycan antibodies. *J Clin Invest*. 1999;104:73–81.
36. Coppo R, Amore A. Aberrant glycosylation in IgA nephropathy (IgAN). *Kidney Int*. 2004;65:1544–1547.

37. Trimarchi HM, Iotti A, Iotti R, et al. Immunoglobulin A nephropathy and ulcerative colitis. A focus on their pathogenesis. *Am J Nephrol.* 2001;21:400–405.
38. Forshaw MJ, Guirguis O, Hennigan TW. IgA nephropathy in association with Crohn's disease. *Int J Colorectal Dis.* 2005;20:463–465.
39. Pouria S, Barratt J. Secondary IgA nephropathy. *Semin Nephrol.* 2008; 28:27–37.
40. McKenzie H, Main J, Pennington CR, et al. Antibody to selected strains of Saccharomyces cerevisiae (baker's and brewer's yeast) and Candida albicans in Crohn's disease. *Gut.* 1990;31:536–538.
41. Peeters M, Joossens S, Vermeire S, et al. Diagnostic value of anti-Saccharomyces cerevisiae and antineutrophil cytoplasmic autoantibodies in inflammatory bowel disease. *Am J Gastroenterol.* 2001;96:730–734.
42. Sutton CL, Yang H, Li Z, et al. Familial expression of anti-Saccharomyces cerevisiae mannan antibodies in affected and unaffected relatives of patients with Crohn's disease. *Gut.* 2000;46:58–63.
43. Landers CJ, Cohavy O, Misra R, et al. Selected loss of tolerance evidenced by Crohn's disease-associated immune responses to auto- and microbial antigens. *Gastroenterology.* 2002;123:689–699.
44. Lodes MJ, Cong Y, Elson CO, et al. Bacterial flagellin is a dominant antigen in Crohn disease. *J Clin Invest.* 2004;113:1296–1306.
45. Dotan I, Fishman S, Dgani Y, et al. Antibodies against laminaribioside and chitobioside are novel serologic markers in Crohn's disease. *Gastroenterology.* 2006;131:366–378.
46. Peyrin-Biroulet L, Standaert-Vitse A, Branche J, et al. IBD serological panels: facts and perspectives. *Inflamm Bowel Dis.* 2007;13: 1561–1566.
47. Suzuki H, Moldoveanu Z, Hall S, et al. IgA1-secreting cell lines from patients with IgA nephropathy produce aberrantly glycosylated IgA1. *J Clin Invest.* 2008;118:629–639.
48. Gasche C, Bakos S, Dejaco C, et al. IL-10 secretion and sensitivity in normal human intestine and inflammatory bowel disease. *J Clin Immunol.* 2000;20:362–370.
49. Philpott DJ, Girardin SE. Crohn's disease-associated Nod2 mutants reduce IL10 transcription. *Nat Immunol.* 2009;10:455–457.
50. Rudd PM, Fortune F, Patel T, et al. A human T-cell receptor recognizes 'O'-linked sugars from the hinge region of human IgA1 and IgD. *Immunology.* 1994;83:99–106.

Glycobiology vol. 22 no. 6 pp. 778–787, 2012
doi:10.1093/glycob/cws012
Advance Access publication on January 30, 2012

N-Acetylglucosaminyltransferase V regulates TGF-β response in hepatic stellate cells and the progression of steatohepatitis

Yoshihiro Kamada[2,3,†], Kanako Mori[2,†], Hitoshi Matsumoto[2,3], Shinichi Kiso[3], Yuichi Yoshida[3], Shinichiro Shinzaki[2,3], Naoki Hiramatsu[3], Mayuko Ishii[2], Kenta Moriwaki[2], Norifumi Kawada[4], Tetsuo Takehara[3], and Eiji Miyoshi[1,2]

[2]Department of Molecular Biochemistry and Clinical Investigation, Osaka University, Graduate School of Medicine, 1-7 Yamada-oka, Suita, Osaka 565-0871, Japan; [3]Department of Gastroenterology and Hepatology, Osaka University, Graduate School of Medicine, Suita, Osaka 565-0871, Japan; and [4]Department of Hepatology, Osaka City University Graduate School of Medicine, Osaka 545-8585, Japan

Received on July 26, 2011; revised on January 17, 2012; accepted on January 25, 2012

N-Acetylglucosaminyltransferase V (GnT-V), catalyzing β1-6 branching in asparagine-linked oligosaccharides, is one of the most important glycosyltransferases involved in tumor metastasis and carcinogenesis. Although the expression of GnT-V is induced in chronic liver diseases, the biological meaning of GnT-V in the diseases remains unknown. The aim of this study was to investigate the effects of GnT-V on the progression of chronic hepatitis, using GnT-V transgenic (Tg) mice fed a high fat and high cholesterol (HFHC) diet, an experimental model of murine steatohepatitis. Although enhanced hepatic lymphocytes infiltration and fibrosis were observed in wild-type (WT) mice fed the HFHC diet, they were dramatically prevented in Tg mice. In addition, the gene expression of inflammatory Th1 cytokines in the liver was significantly decreased in Tg mice than WT mice. Inhibition of liver fibrosis was due to the dysfunction of hepatic stellate cells (HSCs), which play pivotal roles in liver fibrosis through the production of transforming growth factor (TGF)-β1. Although TGF-β1 signaling was enhanced in Tg mouse-derived HSCs (Tg-HSCs) compared with WT mouse-derived HSCs (WT-HSCs), collagen expression was significantly reduced in Tg-HSCs. As a result from DNA microarray, cyclooxygenase-2 (COX2) expression, known as a negative feedback signal for TGF-β1, was significantly elevated in Tg-HSCs compared with WT-HSCs. Prostaglandin E2 (PGE2), the product of COX2, production was also significantly elevated in Tg-HSCs. COX2 inhibition by celecoxib decreased PGE2 and increased collagen expression in Tg-HSCs. In conclusion, GnT-V prevented steatohepatitis progression through modulating lymphocyte and HSC functions.

Keywords: GnT-V / liver fibrosis / steatohepatitis / TGF-β1 / Th1 cytokine

Introduction

Recent findings in glycobiology revealed the direct evidence of the involvement of oligosaccharide changes in human diseases (Ohtsubo and Marth 2006). The branching formation of *N*-glycans is one of the most important factors to regulate biological functions of oligosaccharides in human diseases and is regulated by several kinds of *N*-acetylglycosyltransferases (Zhao et al. 2008). *N*-Acetylglucosaminyltransferase V (GnT-V, gene name; Mgat5) is involved in the synthesis of β1-6GlcNAc formation on *N*-glycans, resulting in increases in the branching formation of *N*-glycan (Taniguchi et al. 1999). It is well known that GnT-V is one of the most important glycosyltransferases involved in cancer metastasis (Lau and Dennis 2008). GnT-V promotes cancer metastasis through the enhancement of growth factor signaling, integrin functions and expression of certain kinds of proteases (Taniguchi et al. 1999, 2001; Lau and Dennis 2008). A study of GnT-V knockout mice also revealed the importance of GnT-V as negative regulators of lymphocytes through modification of T cell receptor oligosaccharides (Demetriou et al. 2001).

In contrast, expression of GnT-V in the normal liver is quite low, but is increased in chronic hepatitis and regenerating liver (Miyoshi et al. 1993, 1995). These results indicate that the up-regulation of GnT-V is the early event of carcinogenesis. GnT-V knockout mice suppressed tumor formation and metastasis after mating with transgenic (Tg) mice of spontaneous cancer development, suggesting that GnT-V is essential in the tumor growth as well as metastasis (Granovsky et al. 2000). To know the direct involvement of GnT-V in carcinogenesis, we have recently established GnT-V Tg mice under control of β-actin promoter (Terao et al. 2011). Although no tumor formation was observed in all organs of GnT-V Tg at 1–2 years after birth, enhanced epithelial–mesenchymal transition (EMT) in the skin was

[1]To whom correspondence should be addressed: Tel/Fax: +81-6-6879-2590; e-mail: emiyoshi@sahs.med.osaka-u.ac.jp
[†]Y.K. and K.M. contributed equally to this work and share first authorship.

observed. Since EMT is a possible event to induce cancer/cancer metastasis, these data prompted us to induce hepatic injury in GnT-V Tg.

Non-alcoholic fatty liver disease (NAFLD) is among the most common causes of chronic liver disease (CLD) in the world, and a growing medical problem in industrialized countries (Ford et al. 2002). A wide spectrum of histological changes has been observed in NAFLD, ranging from simple steatosis, which is generally non-progressive, to non-alcoholic steatohepatitis (NASH), and a proportion of patients with NASH develops cirrhosis and hepatocellular carcinoma (Bugianesi et al. 2002). Recent studies indicate that dietary cholesterol is an important risk factor for the progression of NASH in both human and rodents (Matsuzawa et al. 2007; Yasutake et al. 2009). In addition, cholesterol lowering drugs, such as statins and ezetimibe, were reported to improve NASH progression (Deushi et al. 2007; Hyogo et al. 2008).

In the present study, we treated GnT-V Tg with a high fat and high cholesterol (HFHC) diet and found that overexpression of GnT-V suppressed the development of NASH such as lymphocyte infiltration and liver fibrosis. A possible mechanism was investigated with in vitro experiments, using HSCs in primary culture.

Results

Hepatic injury was attenuated in GnT-V Tg mice compared with wild-type mice fed with the HFHC diet

The body weight was significantly higher in Tg mice than in wild type (WT) ones fed with the normal chow (NC) diet (Table I). In the NC diet-fed mice, the liver weight and liver-to-body weight ratio were significantly higher in Tg ones than in WT ones. In contrast, the liver weight and liver-to-body weight ratio were significantly lower in Tg mice than WT mice fed with the HFHC diet. There were no differences in the serum triglyceride (TG) and cholesterol levels, and liver TG levels between WT and Tg mice fed with the NC and HFHC diets, respectively. There were also no differences in the liver cholesterol contents between Tg and WT mice fed with the NC diet. However, the liver cholesterol levels were significantly lower in Tg mice than in WT ones fed with the HFHC diet.

There were no significant differences in the liver histology between Tg and WT mice fed with the NC diet. However, when mice were fed with the HFHC diet for 4 weeks, the number of infiltrated inflammatory cells in the livers was significantly decreased in Tg mice compared with WT mice (Figure 1A). The majority of these inflammatory cells in the mice livers fed the HFHC diet were CD4- and CD8-positive lymphocytes (data not shown). Serum alanine aminotransferase (ALT) levels were also lower in Tg mice than WT mice fed the HFHC diet (Figure 1B).

Next, we investigated gene expressions of inflammation-related cytokines and chemokines in the mouse livers. When the mice were feeding the NC diet, there were no significant differences in these hepatic gene expression changes. The HFHC diet feeding greatly increased liver inflammatory gene expressions in WT mice. As it was reported that naïve T cells from Mgat5 (GnT-V) knockout mice produce more Th1 cytokines compared with WT cells (Morgan et al. 2004), we investigated the typical Th1 cytokines gene [interferon-γ (IFN-γ), tumor necrosis factor-α (TNF-α), interleukin-6 (IL-6) and IL-1β] expression in the mice livers. We also investigated hepatic nitric oxide synthase 2 (NOS2) and monocyte chemoattractant protein-1 (MCP-1) (CCL2) gene expressions, which are induced by inflammatory stimulation in the NASH liver (Haukeland et al. 2006; Gao et al. 2008). In Tg mice, the inflammatory gene expressions were significantly decreased, compared with WT mice fed with the HFHC diet (Figure 1C).

Liver fibrosis was attenuated in GnT-V Tg mice compared with WT mice on the HFHC diet

To assess liver fibrosis on the HFHC diet, hepatic collagen deposition was evaluated by picrosirius red staining of liver sections. Liver collagen deposition was not different between WT and Tg mice fed with the NC diet, but significantly lower in Tg mice than WT mice fed the HFHC diet (Figure 2A and B). Moreover, hepatic fibrogenic mRNA levels, such as transforming growth factor (TGF)-β, platelet-derived growth factor (PDGF) and collagen Iα1, were significantly lower in Tg mice than in WT mice fed the HFHC diet (Figure 2C).

Table I. Body and liver weights, and biochemical analysis of serum and liver extracts from WT and GnT-V Tg mice fed with the NC or HFHC diet

Diet type	NC		HFHC 4W	
Genotype	WT	Tg	WT	Tg
BW (g)	23.3 ± 0.3	25.6 ± 1.2*	23.1 ± 0.5	26.0 ± 1.5
LW (g)	0.86 ± 0.052	1.09 ± 0.054*	1.52 ± 0.094	1.20 ± 0.075*
LW/BW	0.037 ± 0.002	0.043 ± 0.001**	0.065 ± 0.003	0.046 ± 0.002*
Serum TG (mg/dL)	49.7 ± 2.8	77.8 ± 13.5	23.2 ± 2.8	53.2 ± 12.0
Serum T-cho (mg/dL)	52.1 ± 4.6	66.2 ± 7.7	164.7 ± 12.4	149.6 ± 6.9
Hepatic TG (mg/g liver)	51.0 ± 4.8	55.2 ± 5.2	71.7 ± 5.5	70.3 ± 3.1
Hepatic T-cho (mg/g liver)	19.7 ± 3.0	21.9 ± 1.4	89.0 ± 4.1	61.8 ± 9.0*

BW, body weight; LW, liver weight; LW/BW, liver-to-body weight ratio; TG, triglyceride; T-cho, total cholesterol; NC, normal chow; HFHC, high fat and high cholesterol. Results are the mean ± SEM.

*$P < 0.01$, Tg mice fed the NC diet group vs. WT mice fed the NC diet group.

**$P < 0.05$, Tg mice fed the HFHC diet group vs. WT mice fed the HFHC diet group.

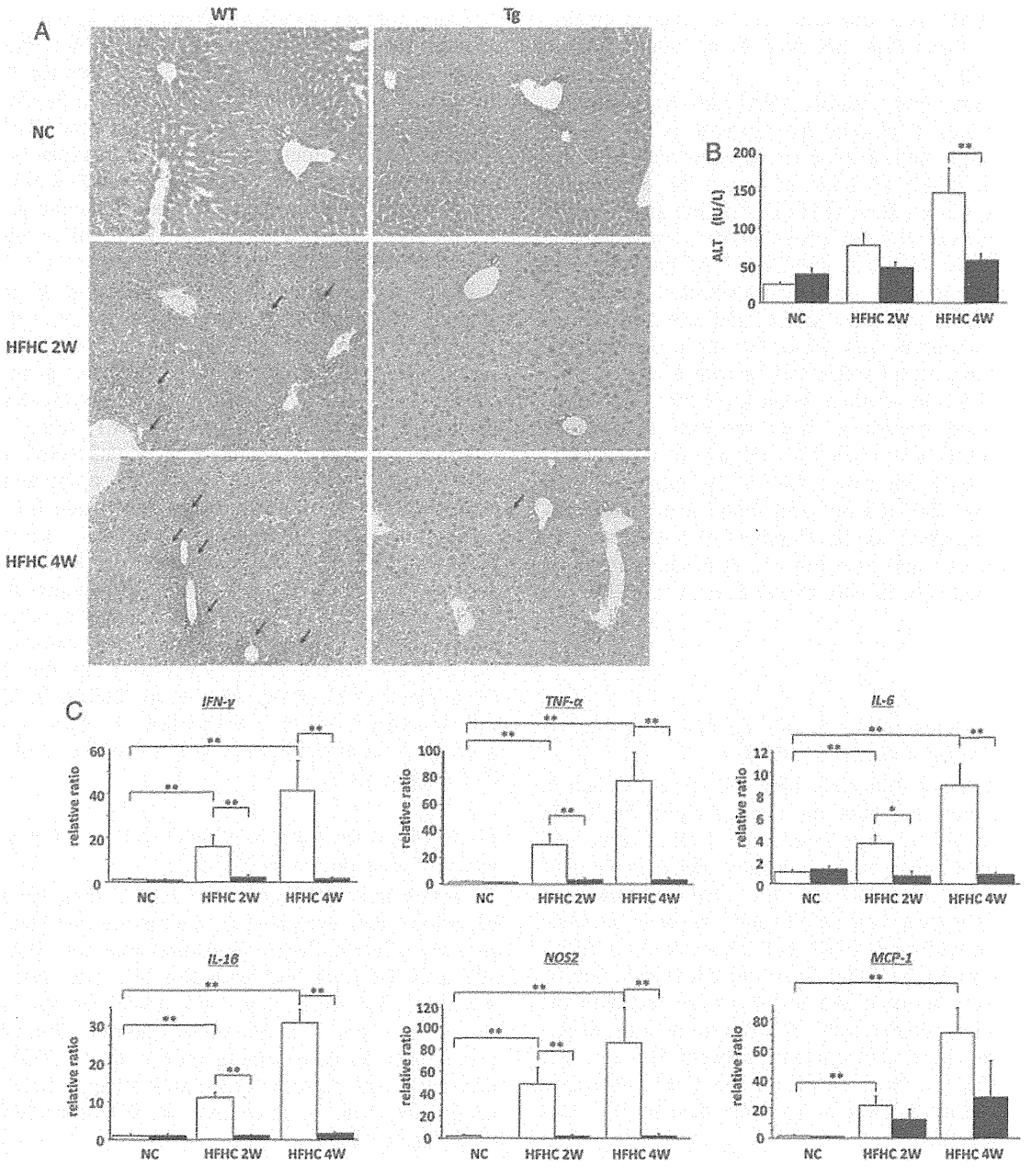

Fig. 1. GnT-V Tg mice developed less serious liver injury than WT mice fed with the HFHC diet. (**A**) Representative photomicrographs of the mice livers of feeding NC or HFHC diet [2 weeks (2W), 4 weeks (4W)] stained with H&E (original magnification, ×200); WT, wild-type mice; Tg, GnT-V Tg mice. Arrows indicate inflammatory cell infiltrations in the mouse livers. (**B**) Serum ALT levels in mice after feeding NC or HFHC diet (for 2W or 4W). (**C**) Hepatic gene expressions in WT and GnT-V Tg mice fed with the NC or HFHC diet. Gene expressions of IFN-γ, TNF-α, IL-6, IL-1β, NOS2 and MCP-1 in the mouse livers were evaluated using real-time RT–PCR. For all panels, bar graphs show the quantification of real-time RT–PCR results. The mRNA expression levels were normalized relative to the level of GAPDH mRNA expression and expressed in arbitrary units. For all panels, white columns indicate WT mice data, and black columns indicate GnT-V Tg mice data. Results are the mean ± SEM ($n = 5$ per group); $^{**}P < 0.01$ and $^{*}P < 0.05$.

Excess expression of GnT-V enhanced β1-6GlcNAc branching of N*-glycans in Tg-HSCs*

L4-PHA binds to the β1-6GlcNAc branching of *N*-glycans, which is the product of GnT-V. To investigate the difference of GnT-V and β1-6GlcNAc branching of *N*-glycans expression in the liver, primary cultured hepatocyte and HSC from GnT-V Tg and WT mice, GnT-V immunoblotting and L4-PHA lectin blotting were performed (Figure 3A–C). GnT-V protein expression was scarcely expressed in WT-HSCs but was increased in Tg-HSCs (Figure 3C, upper panel). The expression of β1-6GlcNAc branching of *N*-glycans (80–200 kDa band) as judged from L4-PHA lectin blotting was significantly increased in Tg-HSCs compared with WT-HSCs (Figure 3C, lower panel, asterisk). In contrast, the expression of GnT-V

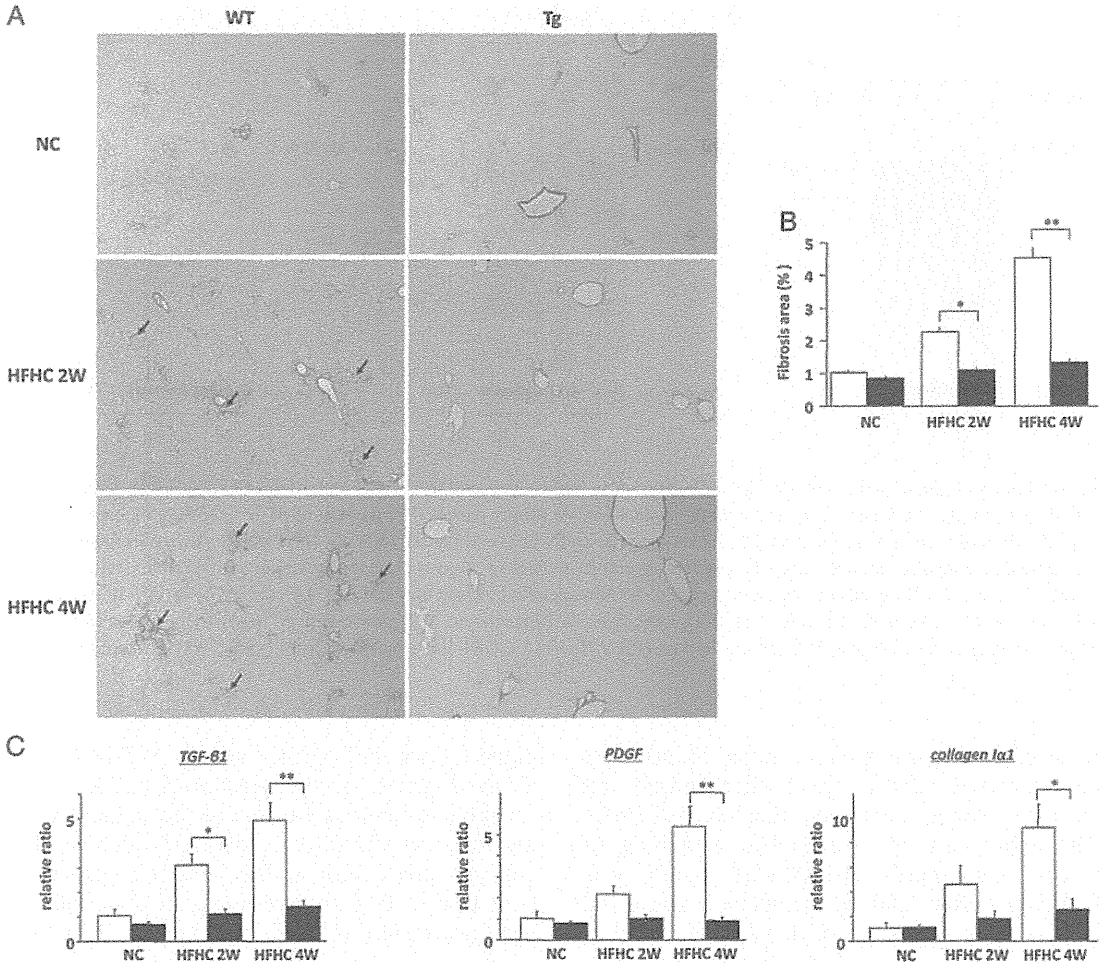

Fig. 2. GnT-V Tg mice developed less serious liver fibrosis than WT mice fed with the HFHC diet. (**A**) Representative photomicrographs of the mice livers of feeding NC or HFHC diet stained with picrosirius red (original magnification, ×100). Arrows indicate the fibrotic area in the livers. (**B**) Histographic representation of quantified data of the fibrotic area in the mice livers. (**C**) Fibrogenic mRNA levels in the mice livers evaluated by real-time RT–PCR. Liver gene expressions of TGF-β1, PDGF and collagen Iα1. The mRNA expression levels were normalized relative to the level of GAPDH mRNA expression and expressed in arbitrary units. For all panels, white columns indicate WT mice data, and black columns indicate GnT-V Tg mice data. Results are the mean ± SEM ($n = 5$); $^{**}P < 0.01$ and $^{*}P < 0.05$ vs. WT mice fed with the HFHC diet group.

was quite low in the livers and hepatocytes in Tg and WT mice (Figure 3A and B, upper panel). Levels of β1-6GlcNAc branching on *N*-glycans were not different despite the aberrant expression of GnT-V. A few differences of L4-PHA bindings in each lane (the liver) might be due to serum contamination.

GnT-V enhanced TGF-β signaling but decreased collagen I expression in Tg-HSCs

To investigate the effect of GnT-V on HSC, we treated WT-HSCs and Tg-HSCs with TGF-β1 (1 ng/mL) and examined fibrosis-related gene expression changes by reverse transcription–polymerase chain reaction (RT–PCR). Treatment of both WT-HSCs and Tg-HSCs with TGF-β1 significantly increased TGF-β1, PDGF and collagen Iα1 expressions. The expression of TGF-β1 and PDGF was increased after 6 h TGF-β1 stimulation and decreased after 30 h. The expression of collagen Iα1 was increased after 6 h in both Tg-HSCs and WT-HSCs and further increased in Tg-HSCs after 30 h. Tg-HSCs showed higher expression levels of TGF-β1 and PDGF with or without TGF-β1 than WT-HSCs (Figure 4A and B). Surprisingly, Tg-HSCs showed a lower expression level of collagen Iα1 than WT-HSCs with or without TGF-β1 (Figure 4C).

To investigate the effect of GnT-V on TGF-β1 signaling in mice HSC, we checked Smad3 nuclear translocation in WT-HSCs and Tg-HSCs after TGF-β1 stimulation (Figure 4D). We could not detect Smad3 nuclear translocation clearly in WT-HSCs after 1 ng/mL of TGF-β1 stimulation (data not shown), so we used 5 ng/mL of TGF-β1 in this investigation. Smad3 protein expression in cytoplasmic extracts of HSCs was decreased after TGF-β1 stimulation, and TGF-β1 stimulation significantly increased nuclear Smad3 protein levels in WT-HSCs and Tg-HSCs. Interestingly, nuclear Smad3 protein levels were significantly higher in Tg-HSCs than WT-HSCs before and after TGF-β1 stimulation. These results indicated that TGF-β1 signaling in mice HSC was enhanced in GnT-V Tg mice.

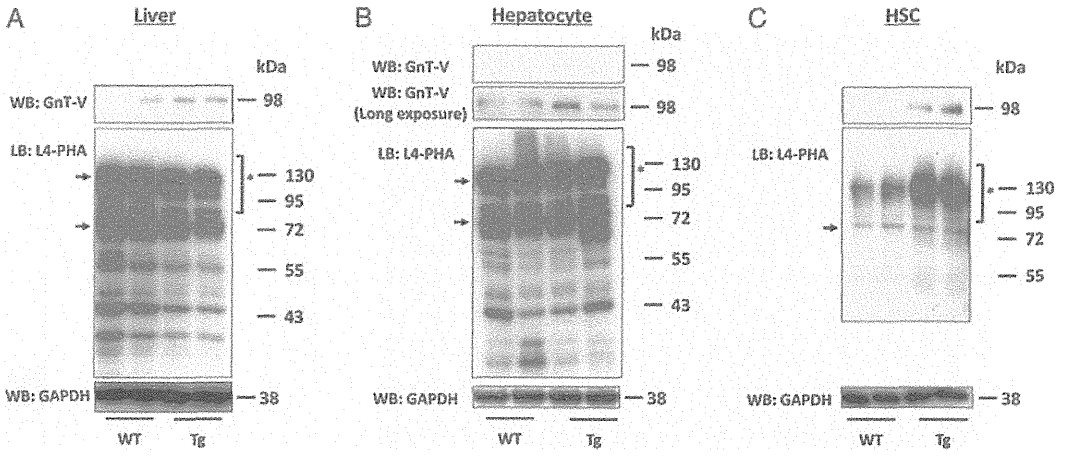

Fig. 3. β1-6GlcNAc structures were increased in GnT-V Tg-HSCs, but not in hepatocytes and the liver. Expression of GnT-V in the liver (**A**), hepatocyte (**B**) and whole cell lysates of HSCs (**C**) were characterized by immunoblot against GnT-V (upper panel). The amount of β1-6GlcNAc branching (the product of GnT-V) was assessed by L4-PHA lectin blot analysis in the liver (A), hepatocyte (B) and whole cell lysates of HSCs (C) (middle panel). Immunoblot against GAPDH (lower panel) was performed as a loading control. Asterisks indicate several β1-6GlcNAc oligosaccharide-containing glycoproteins. Arrows indicate the non-specific bands. The 75- and 130-kDa bands on the blots appear to be non-specific because they are also detected by the avidin-horseradish peroxidase conjugate alone. WT liver, the WT mice liver; Tg-liver, GnT-V Tg mice liver; WT-hepatocyte, WT mouse-derived hepatocyte; Tg-hepatocyte, Tg mouse-derived hepatocyte; HSC, hepatic stellate cell; WT-HSCs, WT mouse-derived HSCs; Tg-HSCs, GnT-V Tg mouse-derived HSCs; WB, western blot analysis; LB, lectin blot analysis.

To determine whether the structures of sugar chains were changed by the increased GnT-V, we further carried out L4-PHA blot analysis using membrane fractions of HSCs (Figure 4E). The expression of β1-6GlcNAc branching of *N*-glycans on cell membrane (80–200 kDa band) was increased in Tg-HSCs before TGF-β1 stimulation compared with WT-HSCs. The expression of β1-6GlcNAc branching of *N*-glycans was elevated after 15 h TGF-β1 stimulation in both WT-HSCs and Tg-HSCs, and its expression was still higher in Tg-HSCs than WT-HSCs. Polylactosamine structures on β1-6GlcNAc branching of *N*-glycans are recognized by endogenous lectins, such as galectins (Lee and Lee 2000; Partridge et al. 2004), and it was also reported that membrane galectins form lattices and lattices forming can inhibit growth factor receptors endocytosis, including TGF-β receptor (Demetriou et al. 2001; Partridge et al. 2004). As expected, weak galectin-3 expression was observed in WT-HSCs, and the expression was elevated in Tg-HSCs compared with WT-HSCs with or without TGF-β1 stimulation. TGF-β1 stimulation elevated cell surface TGF-βR(II) expression in WT-HSCs. In Tg-HSCs, membrane TGF-βR(II) expression was enhanced before TGF-β1 stimulation compared with WT-HSCs, and further elevated after TGF-β1 stimulation. Elevated galectin-3 should inhibit TGF-βR(II) endocytosis, and TGF-βR(II) elevation up-regulated TGF-β1 signaling in Tg-HSCs.

Cyclooxygenase-2 gene expression and prostaglandin E2 production were elevated in GnT-V Tg-HSCs compared with WT-HSCs before and after TGF-β1 stimulation

To investigate the discrepancy between enhanced TGF-β1 signaling and decreased collagen gene expression in mice HSC, we performed DNA microarray analysis between Tg and WT-HSCs (Supplementary data, Table SI). We showed top 30 higher genes in Tg-HSCs than in WT-HSCs. Among various elevated genes, cyclooxygenase-2 (COX2; Ptgs2) is known for the rate-limiting enzyme in prostaglandin E2 (PGE2) production, and COX2-derived PGE2 inhibited TGF-β1-induced collagen production in HSCs as a negative feedback signal (Hui et al. 2004). To investigate the effect of GnT-V on COX2 gene expression of HSCs, we checked COX2 gene expression before and after TGF-β1 stimulation in WT-HSCs and Tg-HSCs by real-time RT–PCR (Figure 5A). Treatment of WT-HSCs and Tg-HSCs with TGF-β1 significantly increased COX2 expressions. Before and after TGF-β1 stimulation, COX2 gene expression was elevated in Tg-HSCs compared with WT-HSCs. In addition, TGF-β1-induced PGE2 production was significantly elevated in Tg-HSCs compared with WT-HSCs (Figure 5B). A selective COX2 inhibitor, celecoxib, treatment significantly decreased PGE2 production and significantly elevated collagen I gene expression in Tg-HSCs (Figure 5C and D).

Discussion

In the present study, we found that murine steatohepatitis progression induced by HFHC diet feeding was prevented in GnT-V Tg mice compared with WT mice. While the enhanced hepatic lymphocytes infiltration and fibrosis were observed in WT mice fed with the HFHC diet, they were dramatically prevented in Tg mice fed with the HFHC diet. Since GnT-V is one of the most important glycosyltransferases involved in carcinogenesis, this result was unexpected. In GnT-V Tg mice fed the HFHC diet, suppression of lymphocytes infiltration was due to a decrease in inflammatory Th1 cytokines in the liver. Inhibition of liver fibrosis in Tg mice was due to the dysfunction of HSCs. In HSCs from GnT-V Tg mice, although TGF-β signaling was enhanced, collagen expression was suppressed.

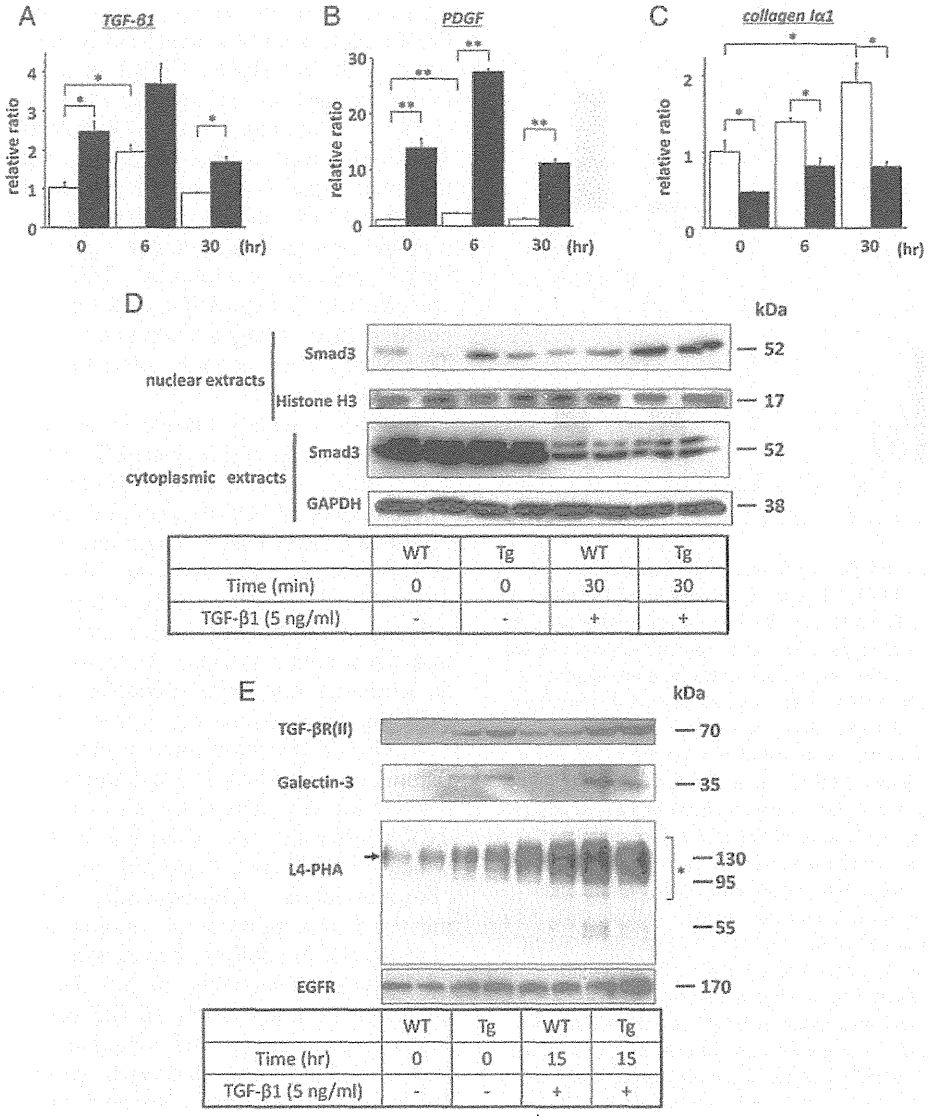

Fig. 4. GnT-V enhanced TGF-β signaling but decreased collagen I expression in GnT-V Tg-HSCs. (**A–C**) Gene expressions in HSCs before and after TGF-β1 stimulation. GnT-V Tg-HSCs and WT-HSCs were stimulated with 1 ng/mL of TGF-β1 for indicated times. HSC gene expressions were assessed using real-time RT–PCR. The mRNA expression levels were normalized relative to the level of GAPDH mRNA expression and expressed in arbitrary units. For all panels, white columns indicate WT mice data, and black columns indicate GnT-V Tg mice data. Results are the mean ± SEM ($n = 5$); $^{**}P < 0.01$ and $^{*}P < 0.05$, vs. the WT-HSC group. (**D**) The nuclear translocation of Smad3 in HSCs before and after stimulation with TGF-β1. Nuclear (upper panel) and cytoplasmic (lower panel) extracts of HSCs were used for immunoblotting of Smad3 before and 30 min after TGF-β1 (5 ng/mL) stimulation. Immunoblots against histone H3 and GAPDH were performed as loading controls. (**E**) GnT-V elevated protein expression of membrane β1-6GlcNAc branching of *N*-glycans, galectin-3 and TGF-βR (II) in activated HSCs. Tg-HSCs and WT-HSCs were stimulated with 5 ng/mL of TGF-β1 for 15 h. The membrane protein of HSCs was extracted and used for immunoblotting. The amount of β1-6GlcNAc branching (the product of GnT-V) was assessed by L4-PHA lectin blot analysis. Immunoblot against EGFR was performed as a loading control. Asterisk indicates several β1-6GlcNAc oligosaccharide-containing glycoproteins. Arrow indicates the non-specific band. Membrane galectin-3 protein and TGF-βR(II) protein expression were evaluated by immunoblotting.

Our study showed that enhanced PGE2 production by elevated COX2 would decrease collagen expression in Tg-HSCs. These findings indicated that GnT-V could prevent steatohepatitis progression in mice.

Growth factor receptors, including TGF-β receptor, are generally *N*-glycosylated transmembrane proteins, and residency at the cell surface is dependent in part on the dynamics of membrane remodeling. Endogenous lectins, such as galectins, generated by *N*-glycan branching can cross-link glycoproteins at the cell surface forming lattices, and galectin binding opposes the loss of receptors to endocytosis (Lee and Lee 2000). Increased cell surface TGF-β receptor is known to enhance the sensitivity to TGF-β1. In GnT-V (Mgat5) knockout tumor cells, cell surface galectin-3 and sensitivity to TGF-β1 was reduced, and chemical endocytosis inhibitor restored the sensitivity to TGF-β1 (Partridge et al. 2004). These findings indicated that galectin forming lattice blocked TGF-β receptor endocytosis and enhanced TGF-β signaling

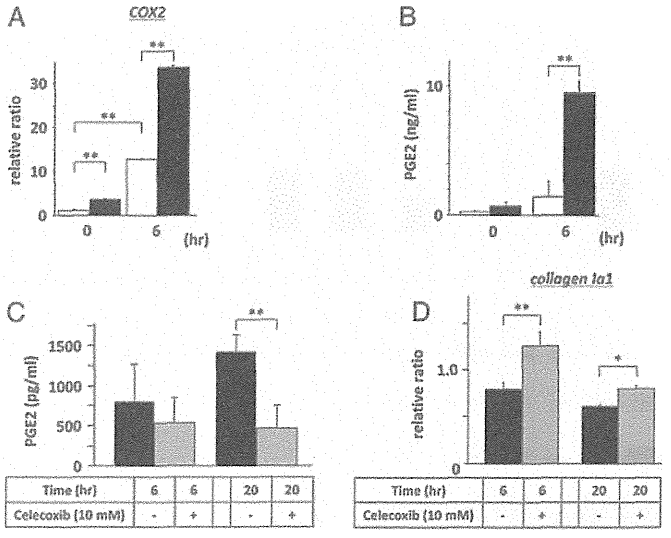

Fig. 5. COX2 gene expression and TGF-β1-induced PGE2 production were elevated in GnT-V Tg-HSCs. (**A**) COX2 gene expressions in HSCs before and after TGF-β1 stimulation. Tg-HSCs and WT-HSCs were stimulated with 1 ng/mL of TGF-β1 for indicated times. HSC gene expressions were assessed using real-time RT–PCR. The mRNA expression levels were normalized relative to the level of GAPDH mRNA expression and expressed in arbitrary units. White columns indicate WT mice data, and black columns indicate GnT-V Tg mice data. Results are the mean ± SEM ($n = 5$); $^{**}P < 0.01$, vs. the WT-HSC group. (**B**) TGF-β1-induced PGE2 production levels secreted into the medium from Tg-HSCs and WT-HSCs were measured by enzyme-linked immunosorbent assay (ELISA). Tg-HSCs and WT-HSCs were stimulated with 1 ng/mL of TGF-β1 for 6 h and before and after TGF-β1 stimulation supernatant of HSCs were collected. Bar graphs show ELISA results and white columns indicate WT mice data, and black columns indicate GnT-V Tg mice data. Results are the mean ± SEM ($n = 5$); $^{**}P < 0.01$, vs. the WT-HSC group. (**C**) PGE2 concentration in medium of Tg-HSCs after celecoxib treatment. Tg-HSC was stimulated with or without 10 mM celecoxib for indicated hours (6 and 20 h), and supernatant of HSC was collected for the measurement of PGE2 by ELISA. Bar graphs show ELISA results and black columns indicate the data of Tg-HSCs without celecoxib treatment, and grey columns indicate the data of Tg-HSCs with celecoxib treatment. Results are the mean ± SEM ($n = 5$); $^{**}P < 0.01$, vs. the non-treated group. (**D**) Collagen Iα1 gene expressions in Tg-HSCs with or without celecoxib treatment. Tg-HSC was stimulated with or without 10 mM celecoxib for indicated times. HSC gene expressions were assessed using real-time RT–PCR. The mRNA expression levels were normalized relative to the level of GAPDH mRNA expression and expressed in arbitrary units. Black columns indicate the data of Tg-HSCs without celecoxib treatment, and grey columns indicate the data of Tg-HSCs with celecoxib treatment. Results are the mean ± SEM ($n = 5$).

(Partridge et al. 2004). As expected, galectin-3 expression and TGF-β signaling (Smad3 nuclear translocation) was enhanced in membrane fractions of HSCs from GnT-V Tg before and after TGF-β stimulation in the present study. As a result, TGF-β1 target gene expressions of TGF-β and PDGF were elevated in Tg-HSCs compared with WT-HSCs. However, collagen Iα1 gene expression, also known for one of TGF-β1 target genes, was significantly lower in Tg-HSCs than in WT-HSCs before and after TGF-β1 stimulation. Furthermore, hepatic fibrosis was attenuated in Tg mice compared with WT mice in vivo. To investigate the reason why collagen expression was decreased in Tg-HSCs in spite of the enhanced TGF-β signaling, we performed microarray analysis between Tg-HSCs and WT-HSCs. Among various elevated genes, COX2 expression was significantly elevated in Tg-HSCs compared with WT-HSCs. COX2 is a rate-limiting enzyme in PGE2 production. It was reported that TGF-β1 stimulated COX2 expression, and COX2-derived PGE2 inhibited TGF-β1-induced collagen production in HSCs as a negative feedback signal (Hui et al. 2004). In this study, celecoxib, a selective COX2 inhibitor, treatment decreased PGE2 production and up-regulated collagen I gene expression in Tg-HSCs. GnT-V-induced continuous TGF-β1 stimulation should enhance COX2 expression, and this negative feedback signal could reduce collagen expression in the Tg mice liver and Tg-HSCs. The precise mechanism for this is under investigation.

TGF-β1 is widely known as an inhibitor of cell proliferation, cell cycle, and activated T cells (Massague 2000; Park et al. 2006; Li and Flavell 2008; Yoshimura et al. 2010). These effects of TGF-β1 should decrease T-cell activation and proliferation and lead to ameliorate steatohepatitis progression in this study. In addition, β1-6GlcNAc branching of *N*-glycans on T-cell antigen receptor (TCR) bind galectins, forming a multivalent lattice that inhibits TCR recruitment into the immune synapse (Demetriou et al. 2001), indicating an inhibitory role for β1-6GlcNAc branching of *N*-glycans in TCR signaling. Moreover, it was reported that naïve T cells from GnT-V knockout mice produce more Th1 cytokines (inflammatory) and less Th2 cytokines (anti-inflammatory) compared with WT cells (Morgan et al. 2004). Agonist-induced TCR clustering was enhanced in GnT-V-deficient T cells, which lowered the threshold for TCR-dependent tyrosine phosphorylation. Consequently, GnT-V knockout mice increased susceptibility to autoimmune diseases (Demetriou et al. 2001). In addition, expression of β1-6GlcNAc branching of *N*-glycans selectively inhibits Th1 cell differentiation and enhances the polarization of Th2 cells (Morgan et al. 2004). In the present study, Th1 cytokines, such as IFN-γ, TNF-α, IL-6 and IL-1β, were decreased in the GnT-V Tg mice liver fed with the HFHC diet compared with WT mice fed with the HFHC diet. These results indicated that β1-6GlcNAc branching of *N*-glycans suppressed Th1 polarization in GnT-V Tg mice and reduced inflammatory cell infiltration in the Tg mice liver.

In conclusion, GnT-V prevented hepatic inflammation and fibrosis in a mice steatohepatitis model through modulating lymphocyte and HSC functions. The enhanced expression of GnT-V in CLDs might protect disease progression as a self-defense reaction.

Materials and Methods

Animal experiments

All experimental protocols described in this study were approved by the Ethics Review Committee for Animal Experimentation of Osaka University School of Medicine.

GnT-V (Mgat5) Tg mice were prepared as described (Terao et al. 2011). WT mice were purchased from Oriental Yeast (Suita, Osaka, Japan). The animals were provided with unrestricted amounts of food and water, housed in temperature- and humidity-controlled rooms and maintained on a 12/12 h

light/dark cycle. The HFHC (containing 15% cocoa butter fat, 1.25% cholesterol and 0.5% cholic acid) and NC diets were purchased from Oriental Yeast.

To determine the role of GnT-V in HFHC diet-induced liver injury, WT and Tg mice (age, 7–9 weeks; sex, male) were assigned to the NC or HFHC diet for 4 weeks. At the end of the experimental period, food was withdrawn for a minimum of 5 h and then the mice were sacrificed. Blood was collected aseptically from the inferior vena cava and centrifuged (2000 g, 7 min, 4°C), and the serum was collected. The liver was either fixed with 10% buffered paraformaldehyde or embedded in compound and frozen at −80°C for histological examination, or immediately frozen in liquid nitrogen for protein and mRNA extraction.

H&E staining and picrosirius red staining

Liver sections were stained with H&E or picrosirius red (Sigma-Aldrich, St Louis, MO). The fibrotic area as a percentage was calculated using image analysis software (winROOF visual system; Mitani Co., Tokyo, Japan).

Determination of gene expression levels

Total RNAs were extracted from whole livers or HSCs with QIAshredder and an RNeasy Mini Kit according to the instructions provided by the manufacturer (Qiagen, Hilden, Germany), and then transcribed into complementary DNA with a Quantitect Reverse Transcription Kit (Qiagen). Quantitative real-time RT–PCR was performed with a QuantiFast SYBR Green PCR Kit using specific primers (Qiagen) on a LightCycler according to the instructions provided by the manufacturer (Roche Diagnostics, Indianapolis, IN). The primers used were IFN-γ (QT01038821), TNF-α (QT00104006), IL-6 (QT00098875), IL-1β (QT01048355), NOS2 (QT00100275), MCP-1 (QT00167832), TGF-β1 (QT00145250), PDGF (QT00266910), collagenIα1 (QT00162204), COX2 (QT00165347) and glyceraldehyde 3-phosphate dehydrogenase (GAPDH; QT00199388) (Qiagen). The mRNA expression levels were normalized as to the GAPDH mRNA expression level and expressed in arbitrary units.

Isolation and culture of mouse hepatocytes and HSCs

Hepatocytes and HSCs were isolated from WT (WT-HSCs) and Tg (Tg-HSCs) mice by two-step collagenase–pronase perfusion of their livers as described previously (Kristensen et al. 2000). Briefly, the livers were perfused for 10 min at room temperature at a flow rate of 3 mL/min with an SC-1 solution [8000 mg/L NaCl, 400 mg/L KCl, 78 mg/L NaH_2PO_4 $2H_2O$, 151 mg/L Na_2HPO_4 $12H_2O$, 2380 mg/L 4-(2-hydroxyethyl)-1-piperazineethanesulfonic acid (HEPES), 350 mg/L $NaHCO_3$, 190 mg/L ethylene glycol tetraacetic acid, 900 mg/L glucose, pH 7.2], followed by digestion at 37°C for 10 min with 0.053% pronase and 0.027% collagenase dissolved in an SC-2 solution (8000 mg/L NaCl, 400 mg/L KCl, 78 mg/L NaH_2PO_4 $2H_2O$, 151 mg/L Na_2HPO_4 $12H_2O$, 2380 mg/L HEPES, 350 mg/L $NaHCO_3$, 735 mg/L $CaCl_2$ $2H_2O$, pH 7.5). Each digested liver was excised and cut into small pieces. The resulting suspension was filtered through a 100-μm cell strainer and centrifuged at 50 × *g* for 1 min at 4°C to obtain hepatocytes. This protocol was repeated three times and then the supernatants were centrifuged at 2000 rpm for 7 min at 4°C. The pellet was washed, suspended in Dulbecco's modified Eagle's medium (DMEM) two times and then plated on a plastic culture dish. The isolated HSCs were maintained at 37°C under 5% CO_2 in DMEM containing 10% fetal calf serum. Isolated hepatocytes were used for further investigation, and HSCs after a few passages were used for the experiments.

HSCs were stimulated with 1 ng/mL of TGF-β1 (Peprotech, Rocky Hill, NJ) for the indicated times. Tg-HSCs were stimulated with 10 mM celecoxib [kindly donated by Phizer Pharmaceuticals (New York, NY)] for the indicated times. RNA extraction and RT–PCR were performed as described in the *Determination of gene expression levels* section.

Western and lectin bolt analyses

Approximately 10 mg of frozen liver tissue was lysed with a lysis buffer [10 mM Tris–HCl, pH 7.4, 150 mM NaCl, 1% NP-40, 0.1% sodium deoxycholate, 0.1% sodium dodecyl sulfate (SDS)]. Isolated mouse hepatocytes were lysed with 1% Triton X-100. For the immunoblotting of nuclear Smad3, HSCs were stimulated with 5 ng/mL of TGF-β1 for 30 min. The nuclear and cytoplasmic proteins of HSCs were extracted and used for immunoblotting of Smad3. For the immunoblotting of TGF-βR(II) and galectin-3, HSCs were stimulated with TGF-β1 (5 ng/mL) for the indicated times. The membrane protein of HSCs was extracted and used for immunoblotting. For lectin blotting of L4-PHA, HSCs were stimulated with TGF-β1 (5 ng/mL) for the indicated times. The membrane proteins of HSCs were extracted and used. Whole cell lysates were prepared by using 1% Triton X-100. A cellular membrane fraction was prepared with Mem-PER (PIERCE, Rockford, IL), according to the manufacturer's instructions. For nuclear and cytoplasmic extracts, cells were lysed in NE-PER extraction reagent (PIERCE) according to the manufacturer's protocol. Samples were then subjected to heat denaturation at 98°C for 5 min. The samples (10–30 μg of protein) were subjected to SDS–polyacrylamide gel electrophoresis and then transferred to a polyvinylidene fluoride membrane. The membrane was subsequently treated with 5% skim milk for western blotting and 3% bovine serum albumin for lectin blotting. Then, for immunodetection, the following antibodies were used: anti-Smad3 antibodies (Cell Signaling Technology, Beverly, MA), anti-TGF-βR(II) antibodies (Santa Cruz Biotechnology, Santa Cruz, CA), anti-galectin-3 antibodies (American Qualex Inc., San Clemente, CA), anti-GnT-V antibody 24D11 (Fujirebio, Tokyo, Japan), L4-PHA lectin (J-Oil Mills Inc. Tokyo, Japan), anti-histon H3 antibody (Cell Signaling Technology), anti-epidermal growth factor receptor (EGFR) antibody (Cell Signaling Technology) and anti-GAPDH antibody (Trevigen, Gaithersburg, MD). Immunoreactive bands were visualized on GE Healthcare film by using ECL detection reagent (GE Healthcare, Waukesha, WI).

PGE2 measurement

PGE2 secreted by HSCs in the presence of TGF-β1 was quantitated using a PGE2 ELISA Kit (Invitrogen, Carlsbad, CA), according to the manufacturer's instructions. HSCs (3×10^5